Distribution Agreement

In presenting this thesis as a partial fulfillment of the requirements for a degree from Emory University, I hereby grant to Emory University and its agents the non-exclusive license to archive, make accessible, and display my thesis in whole or in part in all forms of media, now or hereafter now, including display on the World Wide Web. I understand that I may select some access restrictions as part of the online submission of this thesis. I retain all ownership rights to the copyright of the thesis. I also retain the right to use in future works (such as articles or books) all or part of this thesis.

Tracy M. Eng 25 March, 2022

Effects of Exercise Therapy on Synovial Fluid Inflammation and Joint Tissue Health in Osteoarthritis

by

Tracy M. Eng

Jarred Kaiser
Advisor

Chemistry

Jarred Kaiser

Advisor

David Lynn

Committee Member

Manuela Manetta

Committee Member

2022

Effects of Exercise Therapy on Synovial Fluid Inflammation and Joint Tissue Health in Osteoarthritis

By

Tracy M. Eng

Jarred Kaiser

Advisor

An abstract of
a thesis submitted to the Faculty of Emory College of Arts and Sciences
of Emory University in partial fulfillment
of the requirements of the degree of
Bachelor of Science with Honors

Chemistry

2022

Abstract

Effects of Exercise Therapy on Synovial Fluid Inflammation and Joint Tissue Health in a Post-Traumatic Osteoarthritis Preclinical Model

By Tracy Eng

Introduction: Osteoarthritis (OA) is a debilitating joint disease that leads to cartilage degradation, osteophyte formation and subchondral bone sclerosis. OA is characterized as an inflammatory condition due to cytokine signaling pathways that propagate joint tissue degradation. Exercise is the primary treatment for OA because of its ability to reduce pain and resolve systemic inflammation. However, there are two main caveats that lead to the misunderstanding of exercise's effectiveness against OA: (1) differential exercise parameters used in pre-clinical and clinical testing leads to varying results in exercise's therapeutic outcomes and (2) patient non-compliance prevents the realization of the long-term effectiveness of exercise. This thesis sought to standardize an exercise therapy regimen for a preclinical model to demonstrate the positive effects of exercise on joint tissue health. This exercise therapy was then applied to observe how various synovial cytokine levels may be altered with therapeutic exercise to identify potential pharmaceutical targets that could provide the benefits of exercise while overcoming the barrier of patient non-compliance. We hypothesized that a low-moderate exercise therapy would slow joint degradation and resolve intra-articular inflammation in a preclinical OA model.

Materials and Methods: A literature search of twenty-five (n=25) articles was conducted to determine the parameters of our preclinical exercise regimen. Medial meniscal transection (MMT) surgeries were performed on male Lewis rats to induce OA. Exercise groups performed mild treadmill walking for 30 min/day, 5 days/week at 10 m/min for 3 weeks, starting 3 weeks after surgery. Cartilage, osteophyte, and subchondral bone morphology of the medial tibia were analyzed with EPIC-micro CT. Spatiotemporal symmetry of gait was collected using EDGAR. Nineteen (n=19) inflammatory cytokines within the synovial fluid were measured and standardized using a multiplex ELISA array.

Results: MMT resulted in the development of OA, yet our established exercise protocol was able to improve both individual tissue morphological characteristics and overall tissue health in the MMT models. Exercise also maintained spatiotemporal symmetry. MMT altered synovial cytokine fluid levels, in which our exercise regimen was able to restore. Lead cytokines for morphological variation between exercised and non-exercised OA groups were IP-10 and IL-10, such that they accounted for 44% of the variability. Higher IP-10 levels were correlated with an anti-sclerotic response of the subchondral bone. IL-10 levels were positively associated with greater areas of exposed bone and osteophyte formation.

Discussion: Based on a literature search, we established an exercise regimen using mild treadmill walking to maintain joint tissue health, spatiotemporal symmetry, and intra-articular inflammation in a pre-clinical OA model. IP-10 and IL-10 were identified as lead cytokines in regulating cartilage breakdown, osteophyte formation and subchondral bone remodeling with respect to exercise. These findings demonstrate how therapeutic exercise can reduce intra-articular inflammation overall and how specific cytokine levels may dictate joint morphological changes.

Clinical Relevance: Exercise can slow disease progression of OA by shifting intra-articular cytokine levels back to a normal state. IP-10 and IL-10 level regulation could lead to a better understanding of exercise's ability to reduce tissue degradation in OA.

Effects of Exercise Therapy on Synovial Fluid Inflammation and Joint Tissue Health in a Post-Traumatic Osteoarthritis Preclinical Model

By

Tracy Eng

Jarred Kaiser

Advisor

A thesis submitted to the Faculty of Emory College of Arts and Sciences
of Emory University in partial fulfillment
of the requirements of the degree of
Bachelor of Science with Honors

Chemistry

2022

Acknowledgements

I would like to especially thank my research advisor, Dr. Jarred Kaiser, for his endless support in all my endeavors. In addition to helping me complete this project, his mentorship has helped me find an area I am passionate about and want to pursue in the future.

I would also like to thank both Dr. Nick Willett and Dr. Hicham Drissi for opening their doors to me and allowing me to grow as a researcher in their labs.

Thank you to my committee member, Dr. David Lynn, for teaching me to think about the singer and not the song. Grazie to my other committee member, Dr. Manuela Manetta, for her unconditional support and for always making me smile.

Table of Contents

1. Introduction

1.1 Knee Joint Anatomy and Physiology

The knee is a hinge joint where the tibia, fibula and femur meet, connecting the lower and upper parts of the leg.[1] It is classified as a synovial joint, which is defined by the synovial tissue and fluid aiding in the articulation of the joint (Figure 1). The synovial fluid provides both lubrication between the bones and nourishment to the articular cartilage, especially because cartilage lacks blood vessels.[2] The synovium is the connective tissue that lines the joint capsule, providing structural support to the joint and controlling nutrient exchange between the blood and synovial fluid.[3,4] The synovial tissue consists of two main cell types: macrophage-like synoviocytes (MLS) and fibroblast-like synoviocytes (FLS). The primary role of MLS are to maintain joint homeostasis by phagocytosing cellular debris and waste.[5] FLS produce proteins, including hyaluronan, fibronectin, lubricin and collagen, to enhance the lubricative properties of the synovial fluid in addition to providing structural protein materials to the cartilage.[6]

Another key feature of the knee joint are the thin layers of cartilage that cover the articulating surfaces of the tibia and femur. The main function of this cartilage is to prevent the two bones from rubbing against one another.[7] Structurally, the articular cartilage consists of an extracellular matrix (ECM) that is primarily composed of chondrocytes, water, collagen, and proteoglycans.[8] Chondrocytes are cells distributed throughout the cartilage that produce, maintain, and repair other components of the ECM. The ECM consists of different zones, such that each zone has a different protein and cellular organization.[9] Driven by interactions between the ECM elements, cartilage maintains its specific biomechanical properties, which allow it to evenly distribute the intense loads of the knee.[8]

Beneath the articular cartilage is the subchondral bone, which supports cartilage homeostasis both biomechanically and biochemically. Cartilage and subchondral bone crosstalk occurs by the regulation of the dynamic subchondral bone structure and the secretion of growth factors between the two tissues.[10, 11] The structural make up of bones are primarily regulated by three cell types: osteoblasts, osteoclasts, and osteocytes. Osteoclasts and osteoblasts are responsible for bone resorption and bone formation, respectively, playing a significant role in regulating the volume and density of the subchondral bone. Osteocytes lie within the bone and play a key role in regulating osteoblast activity.[12,13] Thus, the knee is a complex system, in which cellular activity of its tissues contribute to joint homeostasis.

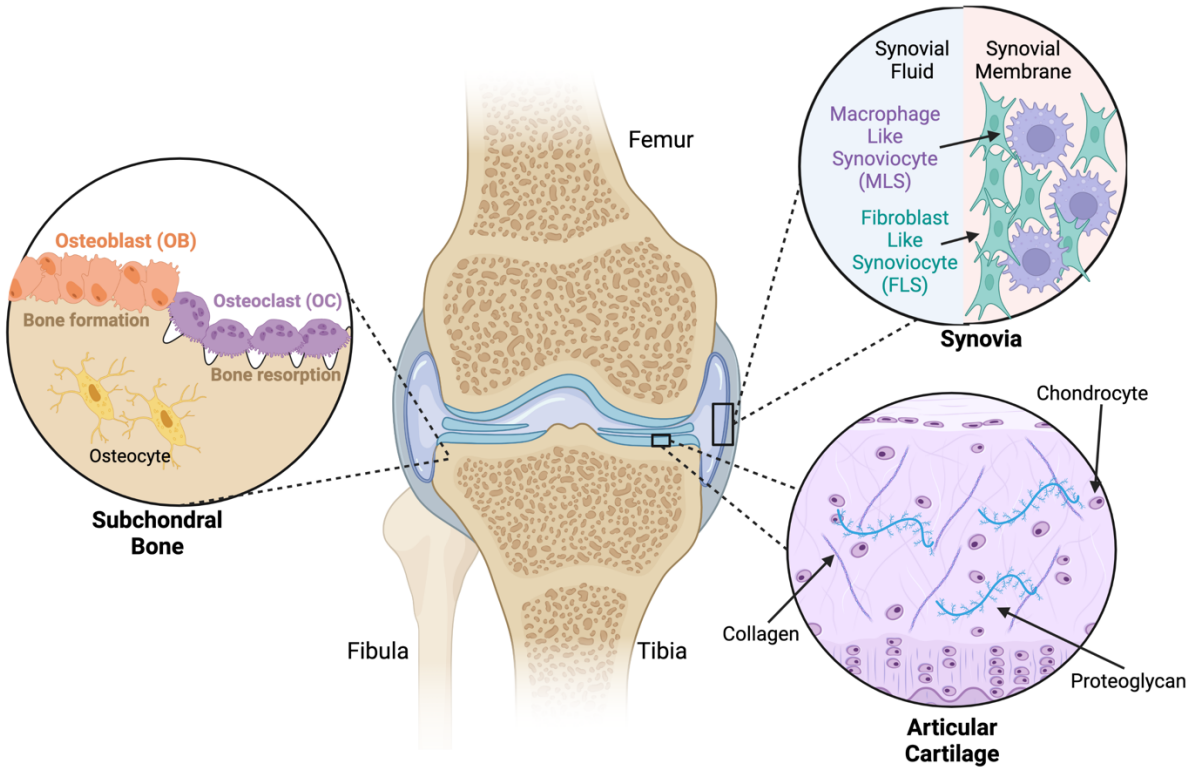

Figure 1. The knee joint consists of various tissue components, including the synovium, articular cartilage, and subchondral bone. The synovia is comprised of the synovial fluid and a synovial membrane surrounding the fluid. The connective tissue of the synovial membrane contains two main cell types: macrophage-like synoviocytes (MLS) and fibroblast-like synoviocytes (FLS). Covering both the femur and the tibia is articular cartilage, which is formed by an extra-cellular matrix (ECM). The cartilage ECM contains proteins, chondrocytes, and water. Directly beneath the articular cartilage is the subchondral bone, whose structure is maintained by three main cell types: osteoblasts, osteoclasts, and osteocytes. (Made on Biorender).

1.2 Osteoarthritis

Osteoarthritis (OA) is a debilitating joint disease that affects over 32.5 million adults in the U.S., most commonly affecting the knee.[14] OA disturbs the whole joint through biochemically mediated interactions between the joint tissues (Figure 2).[15] OA initiation varies across disease phenotypes, with aging and injury being the most common causes for OA development. OA is propagated through the breakdown of the cartilage ECM and elevation of synovial inflammation, leading to alterations in knee function. Additionally, subchondral bone remodeling, including thinning and thickening of the bone, also contributes to the joint's inability to evenly distribute loads. [16] Hence, OA is a complex disease affecting the whole joint, and is due to the interactions between the joint's tissues.

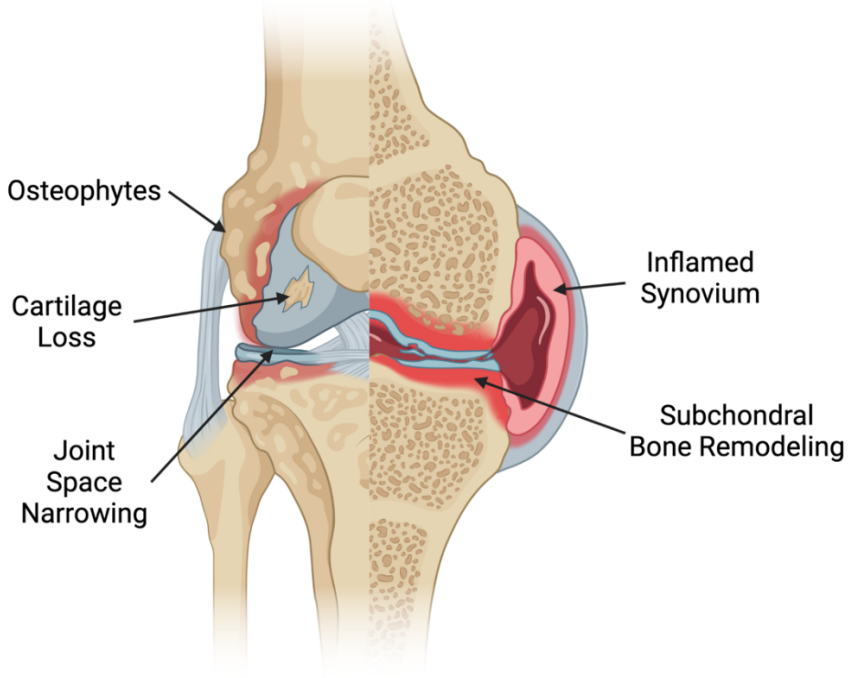

Figure 2. Osteoarthritic knee joint as characterized by articular cartilage loss, subchondral bone sclerosis, osteophyte formation and intra-articular inflammation. OA is a complex whole joint disease propagated by the deterioration of the joint's multiple tissue components. (Made on Biorender).

Inflammation within the joint plays a key role in the progression of OA (Figure 3). The imbalance of pro-inflammatory cytokines, or signaling molecules, versus anti-inflammatory cytokines help drive the degradation of the joint's tissues.[17] Pro-inflammatory cytokine signaling

upregulates the breakdown of cartilage by elevating the proteolytic activity of matrix metalloproteinases (MMPs). These activated MMPs digest proteins in the ECM, most commonly type II collagen and aggrecan.[18,19] Fragments of the broken ECM bind to the membranes of synoviocytes, triggering the activation of downstream pro-inflammatory cascades, including the increased expression of tumor necrosis factor – alpha (TNF-α) and interleukin-1-beta (IL-1β), both pro-inflammatory cytokines. TNF-α and IL-1β then bind to chondrocytes triggering the production of more MMPs, specifically MMP-13 and MMP-3, accelerating cartilage breakdown. The pathogenesis of OA is a vicious cycle that is escalated by the increase of synovial inflammation and MMP breakdown of the ECM. [20,21]

Remodeling of the subchondral bone is also stimulated by the imbalance of inflammatory regulation, mostly in part by the interactions between the bone and cartilage. Bone marrow lesions are the first signs of bone degeneration and are speculated to be a reparative response to mechanical overloading on the joint. Subchondral bone remodeling occurs following bone marrow lesion formation, resulting in increased bone volume, but also a loss in bone mineral density. [22] Inflammation plays a significant role in subchondral bone remodeling because, during the breakdown of articular cartilage, osteoblasts express pro-inflammatory phenotypes. This increased inflammatory cytokine signaling facilitates subchondral bone sclerosis, or the thickening of the bone, and the further breakdown of the cartilage ECM by activating chondrocyte production of MMP-13 and MMP-3. [23,24] Similarly, when the knees are unable to equally distribute loads, subchondral bone micro-fractures begin to form. Bone marrow osteocytes respond to these fractures with the expression of apoptotic signals and increased inflammation causing elevated bone resorption by osteoclasts.[25]

Another morphological feature that occurs during OA is osteophyte development, which are bony and cartilaginous growths found at the margins of the articular cartilage (Figure 2). Osteophyte formation occurs from the differentiation of mesenchymal cells (MSC) in the periosteum, or the membrane lining the outside of bones. Proliferation of these MSC is likely in response to synovial inflammatory signaling, such that osteophyte formation acts as a repair mechanism to stabilize the knee following cartilage breakdown. Nonetheless, stabilization of the joint is often not observed since osteophytes are associated with stages of OA involving pain and loss of joint mobility. [26]

Furthermore, the interactions between the synovial membrane and the immune system contributes to the exaggerated inflammation within the joint upon articular cartilage breakdown. As noted, one of the key pathways in OA pathogenesis is when MMPs digest ECM proteins and the protein fragments are phagocytosed by macrophage-like synoviocytes (MLS). This particularly results in the activation of the NF-kB pathway, a pro-inflammatory pathway that organizes responses to pathogens. The NF-kB pathway is responsible for TNF-α and IL-1β being secreted into the synovial fluid by activated MLS. [27, 28] However, the elevated levels of pro-inflammatory signaling molecules also leads to the recruitment of T-cells, neutrophils, and macrophages into the synovial joint. This further promotes a pro-inflammatory environment in addition to the already activated inflammatory pathways.[29] Immune cell inflammation promotes articular cartilage loss, subchondral bone remodeling and osteophyte formation.[30 ,31] Therefore, expanding our knowledge of synovial inflammation through cytokine signaling can elucidate a better understanding for how OA progresses and how it can potentially be treated.

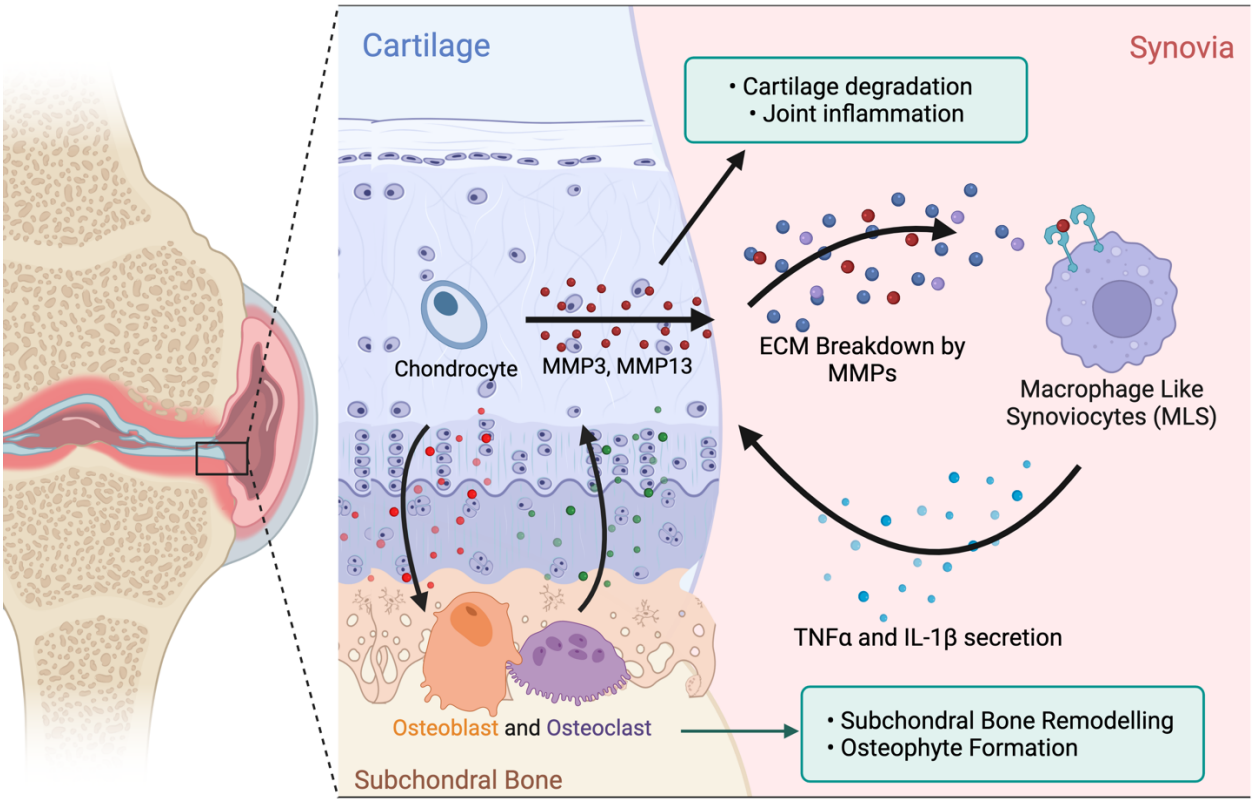

Figure 3. Role of Inflammation in OA. Cytokine mediated pathways lead to cartilage degradation, joint inflammation, subchondral bone sclerosis, and osteophyte formation. Crosstalk between different tissues leads to deterioration of the whole joint. (Made on Biorender).

Preclinical *in vivo* models offer a powerful tool to study OA treatment because of our ability to analyze the mechanisms of OA on a cellular level at a specific stage in the disease of a living organism. Various rodent models have already been developed to simulate the progression of OA using either biochemical injections or surgical induction.[32] In addition, rodents have a similar knee anatomy to humans but also accelerated timelines for OA pathogenesis. Fortunately, preclinical rodent models can be used to study synovial inflammation and morphological joint degradation, allowing us to elucidate biochemical mechanisms that link these two processes of OA pathogenesis in a living organism.

1.3 Exercise Therapy Effectiveness Against OA

Currently there are no FDA-approved disease modifying drugs available in the clinic to treat OA. Physical exercise is one of the only OA interventions to reduce pain and ameliorate joint tissue degeneration.[33] In fact, exercise therapy is proposed to reduce systemic pain sensitivity through the development of central nervous system adaptations.[34] Exercise also reduces systemic inflammation by attenuating TNF-α production, which was observed in adults following a 12-week aerobic training program.[35] Pain and inflammation are interconnected with respect to OA because peripheral pain sensitization is likely due to elevated inflammation in the joint. This suggests how controlling such joint inflammation through exercise therapy can mitigate OA associated peripheral pain sensitivity.[36,37] Hence, exercise offers a promising therapy for OA through its potential ability to control inflammation and mitigate systemic and peripheral pain.

In studying the dynamic effects of exercise therapy on OA, preclinical rodent models are primarily used. Such models utilize treadmill walking, wheel running and applied mechanical loading. Many of these pre-clinical models have already demonstrated the beneficial effects of exercise treatment on OA. For example, moderate physical exercise with normal joint loading improved the lubrication and cartilage preservation in elderly rats by increasing lubricin synthesis in the synovial fluid.[38] Mild treadmill walking in a preclinical model enhanced ECM synthesis and repair through the elevated expression of bone morphogenetic proteins (BMPs). BMP upregulation led to reduced cartilage degeneration, minimized osteophyte growth, and less subchondral bone remodeling following exercise treatment.[39] Mechanical stress from treadmill exercise also reduced sensitization to the NF-kB pathway in adult rats, regulating chondrocyte and synoviocyte inflammatory signaling.[40] Additionally, voluntary wheel running of rats reduced

pain and stress related behavior following the induction of paw inflammation.[41] Overall, preclinical exercise models mimic the pain and inflammatory sensitivity results in clinical models, while also demonstrating positive effects on tissue health. These findings indicate exercise's potential role in treating OA on both the macroscopic and cellular levels.

1.4 Exercise, Inflammation and Joint Tissue Health

One of the main gaps in research conducted on exercise's effects against OA is the connection between exercise, local inflammation, and joint tissue health. At the molecular level, exercise is a powerful regulator of systemic inflammation through cytokine signaling and immune system response regulation.[36] Following skeletal muscle contraction, muscle fibers secrete interleukin-6 (IL-6) into the bloodstream, causing the downstream inhibition of TNF-α and IL-1β.[34] Exercise also suppresses pro-inflammatory cytokine levels by controlling immune cell populations in the synovia. In particular, exercise induces systemic macrophage polarization towards the M2 anti-inflammatory phenotype and increases the circulation of regulatory T cells.[42,43,44,45] Although these findings demonstrate the positive effects of exercise on the body's overall inflammatory response, localized inflammation within the knee joint should be further examined to understand how exercise affects joint tissue health through cytokine signaling.

1.5 Caveats of Studying and Applying Exercise Therapy to OA

A primary problem in studying exercise therapy in preclinical models is that there has been no consistent regimen of exercise that longitudinally supports its benefits on inflammation and joint tissue health. Rather, variations between studies have resulted in the idea that exercise and mechanical loading have differential results on joint preservation and/or degradation. In one pre-clinical incline treadmill running regimen, exercise resulted in increased cartilage matrix degradation and osteophyte formation.[46] In contrast, a much less intense exercise regimen also

using treadmill walking led to the preservation of proteoglycans.[47] Variation in intensity, duration, and onset of exercise therapy has led to contradictory results in exercise's ability to reduce OA progression. Thus, identifying exercise therapy parameters that are associated with the reduction of inflammation and joint degeneration remains an important step in identifying how exercise affects the joint on the molecular level.

Furthermore, although exercise has exhibited great benefits on preserving tissue health, the other major pitfall of exercise therapy is patient adherence to their respective programs. In a study on exercise therapy for OA patients, only 57.8% of the sample were adherent to their exercise program after 3 months. These percentages steadily declined to 44.1% and 30.1% following 15 and 60 months, respectively.[48] Therefore, the long-term effectiveness of exercise interventions is often not realized due to the lack of patient compliance to exercise programs. A potential solution to this problem is to develop a pharmaceutical intervention that can elicit the same positive biochemical effects that follow long-term exercise treatment. Identifying the molecular mechanisms associated with exercise therapy and the reduction of inflammation could inform the design of an "exercise injection" that provides the same therapeutic outcomes of exercise, while overcoming the barrier of patient compliance.

1.6 Objectives and Significance

The goal of this thesis was to identify biochemical associations between synovial inflammation and joint tissue health during exercise treatment of OA. To achieve this goal, I had two specific aims. The first aim was to develop a therapeutic pre-clinical exercise OA model. I then aimed to classify the intra-articular synovial fluid cytokines associated with this developed exercise therapy and the improvement of joint tissue health. I hypothesized that a low-moderate exercise regimen can slow tissue degradation and reduce intra-articular inflammation.

2. Materials and Methods

Aim 1: Develop a Preclinical Exercise Therapy Model for Post-Traumatic OA

2.1 Preclinical Exercise Model Literature Review

A literature search was conducted using an electronic database (Google Scholar). Keywords for the search included: osteoarthritis, arthritis, knee, exercise, physical therapy, rats, mice, mouse, preclinical model, running, treadmill, applied loading, walking, cartilage, exercise program, and physical activity. Studies conducted on preclinical rat and mouse models were eligible for inclusion. Exercise therapy for OA included treadmill walking, incline running, and voluntary wheel running.

A total of twenty-five (n = 25) full journal articles were obtained from the literature search (SI 1). The species being studied, the OA induction method, exercise treatment, onset of exercise, intensity of exercise, exercise dosage per day and week, duration of the exercise regimen, and the effects on pain and joint tissue health were collected from each article. The onset of exercise was defined as when the exercise therapy first began, including either prior or after OA induction. Intensity was considered as the speed of the walking/running. All values for the dosage of exercise per day and week were normalized to the total of min/week (min/wk) of exercise for each regimen.

We then characterized the effect of exercise on joint tissue health and pain/function. Studies reported a variety of pain outcomes including weight bearing symmetry, von Frey testing, and thermal hypersensitivity. Joint tissue health outcomes included degenerative changes to the articular cartilage, subchondral bone remodeling, intra-articular inflammation, and osteoclast differentiation using tools such as micro-computed tomography and histological staining. A score of +1 was given if exercise improved tissue health/pain, a score of 0 was

assigned if exercise did not affect outcomes, and a score of -1 was named if exercise worsened outcomes.

2.2 Exercise Regimen Determination

All data extracted from the literature search was collected and analyzed using JMP® Pro 16.0.0. For our implementation of exercise therapy, we decided to cap therapies to a reasonable intervention time (30 min/d for 5 d/wk) in order to reduce the design parameter space. The specified dosage was plotted against intensity, duration and onset using contour plots (Figure 4). Contours indicated associations between the dosage and exercise regimen parameters with respect to tissue health. For example, the intensity of the exercise therapy (velocity of walking in m/min) was extracted by identifying our specified dosage per week (150 min/wk) on the horizontal axis. We then identified where 150 min/wk corresponded to tissue improvement (green contours). The intensity was determined as the minimum value on the y-axis that was in line with the lowest point on the contour. In other words, the minimum intensity associated with both positive tissue changes and 150 min/wk was collected as our identified parameter. The same technique was used to determine the minimum duration of the therapy and the latest time of onset for exercise.

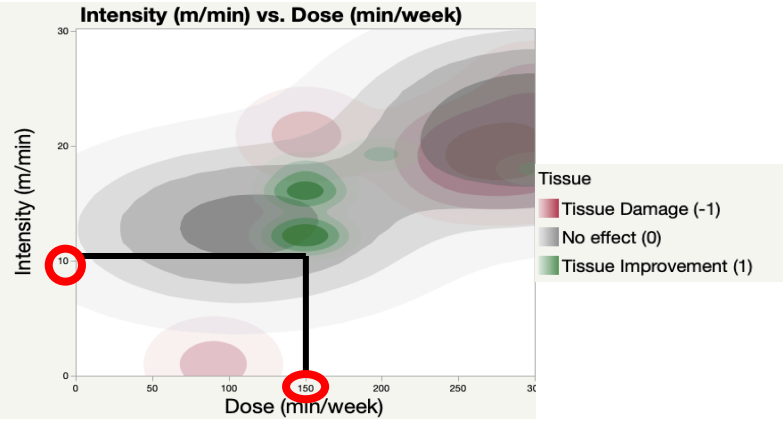

Figure 4. Example contour plot for the determination of exercise intensity for our developed exercise therapy. Colored contours were used to indicate tissue health changes, with red being associated with tissue damage, gray having no effect and green improving tissue health. For all parameter identification processes, 150 min/wk was used as our specified dosage.

2.3 Preclinical OA Model Development

All animal care and experiments were performed in accordance with the Atlanta Veteran Affairs Medical Center's (VAMC) institutional guidelines. Experiments were approved by the Atlanta VAMC Institutional Animal Care and Use Committee (IACUC) (Protocol: V002-18).

Twenty-four (n = 24) male Lewis rats (Strain Code: 004, Charles River) were acclimated to treadmill walking to identify trainability before surgeries. All animals were placed on a stationary treadmill for 25 minutes in the dark, and then walked for 5 minutes at 10 m/min. Acclimation continued for an additional 5 days, with a 5-minute increase in exercise duration each subsequent day, resulting in a total of 30 min/d on the last day of acclimation. Trainability was defined as the ability to walk for the full length of the exercise routine each day. An air stimulus was used to encourage movement, if needed. Following acclimation, approximately fifteen percent (~15%) of the animals were excluded because of lack of trainability. These animals were randomized into the non-exercised treatment groups. The remaining animals were then randomly divided across all the treatment groups.

OA was induced using a rat medial meniscal transection (MMT) surgery on the left hind leg as described by Bendele, 2001.[49] Prior to surgery, all animals were anesthetized using isoflurane. SR buprenorphine (ZooPharm, Windsor, CO) was subcutaneously administered as an analgesia. All surgeries were initiated by creating an incision along the medial side of the animal's left hind knee to expose the tibial-femoral joint. For MMT surgeries, medial collateral ligaments (MCLs) were exposed by performing a blunt dissection. MCLs were then cut to further expose the medial meniscus. Menisci were transected at the narrowest point (Figure 5). Soft tissues were sealed with 4.0 vicryl sutures and wounds were closed using surgical staples. Sham surgeries were performed in the control groups and were done by dissecting the MCL

only. All animals were monitored during a three-day post-operative period to ensure recovery. Surgical staples were removed seven days following surgery. For specificity, controls were identified as Sham (Sham and Sham + Exercise) and OA induced animals were called MMT (MMT and MMT + Exercise).

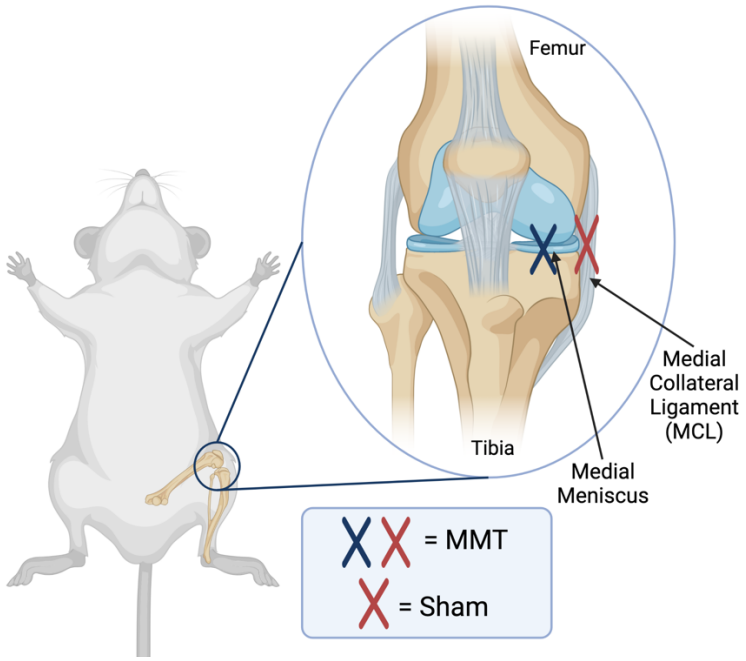

Figure 5. Schematic of Sham and Medial Meniscal Transection (MMT) Surgeries. Sham surgeries consisted only of the blunt dissection of the MCL. MMT surgeries included both the transection of the MCL and the medial meniscus. (Made on Biorender).

2.4 Exercise Therapy

All exercise groups (Sham + Exercise and MMT + Exercise) began their exercise therapy three weeks (n = 21 days) following surgery. Animals walked on the treadmill for 30 min/d at 10 m/sec for 5 d/wk. Exercise regimens continued for a total of three weeks. Animals in the non-exercise groups (Sham and MMT only) did not receive any additional treatments. Animals were free to move about their cages when not undergoing treatment. All rats were euthanized 6 weeks post-surgery using CO_2 asphyxiation when moderate post-traumatic OA was expected. (Figure 6).

2.5 Gait Analysis

Spatiotemporal symmetry of gait was measured using the Experimental Dynamic Gait Arena for Rodents (EDGAR). All animals were acclimated to the gait arena for 3 days before baseline testing was performed. Gait data was collected prior to surgery and 2-, 4- and 5-weeks following surgeries. The gait arena consisted of a 60" x 10" transparent cage, such that when animals freely moved across the enclosure, paw placement along the cage floor could be observed. Videos of the sagittal and ventral planes of the animals were captured using a high-speed camera as they crossed the cage (Phantom Miro 320, Vision Research, Inc.). Animals were allowed to explore the cage, until a total of 10 right and left foot strikes were recorded. All videos were processed using the EDGAR software package, utilizing MATLAB (MathWorks), to calculate velocity, stance times, stride times, imbalance, step widths, stride length, and spatial/temporal symmetries.

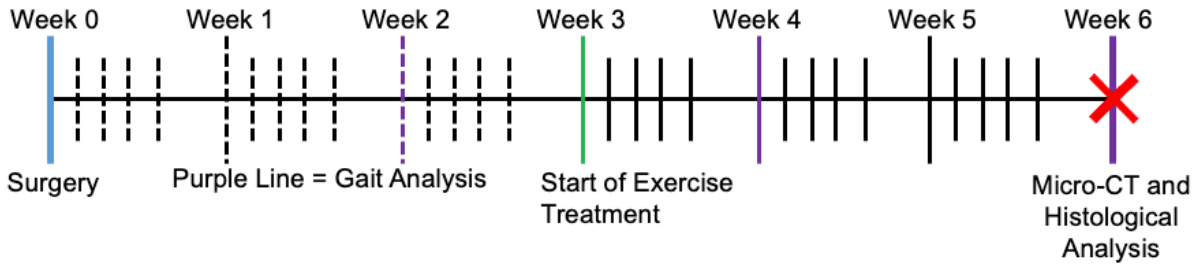

Figure 6. Timeline of Aim 1 Experiments. Surgeries were indicated as Week 0. Exercise treatment began 3 weeks (21 days) following surgery and continued for an additional 3 weeks (Solid lines). Gait analysis was performed prior to surgery and 2-, 4- and 5-weeks following surgery (Purple Lines).

2.6 Micro-CT and Histological Analysis

Knee joint morphology was quantified using Equilibrium partitioning of an ionic contrast agent (EPIC) micro-CT scanning. Following euthanasia, left hind limbs were harvested, fixed in formalin, and carefully dissected to expose the articular cartilage surface of the tibia. Prior to scanning, the tibia was immersed in 30% Hexabrix® 320 contrast reagent and 70% phosphate

buffer saline (PBS) for 30 min at 37° C. All tibiae were scanned using Scanco microCT 40 (Scanco Medical).

Coronal sections of the tibiae were contoured to evaluate articular cartilage, subchondral bone, and osteophytes. Contouring for articular cartilage and subchondral bone were performed across the entire medial tibiae and the medial-most third. Parameters collected included: tissue volume, thickness, porosity, and attenuation. Cartilage attenuation was inversely proportional to the concentration of glycosaminoglycans (GAGs). Subchondral bone attenuation was associated with the mineral density of the bone. Osteophyte volumes were evaluated on the medial side of the tibia and were characterized as cartilaginous or mineralized.

Surface roughness and cartilage loss were analyzed by exporting 2D grayscale images from the micro-CT scans and importing them to MATLAB. A custom algorithm generated 3D representations of the cartilage surfaces and then fit a 3D polynomial along the generated cartilage surface. Surface roughness was evaluated by calculating the root mean square of differences between the 3D cartilage surface and 3D polynomial.

2.7 Statistical Analysis of Aim 1

Independent parameters and overall gait and tissue morphology were analyzed as dependent variables using partial least squares regression (PLSR) with the four different treatment groups as independent variables. Measurements were reduced to three latent variables (LV). The first and second LVs were rotated to maximize the difference between independent variables. Significant differences between the four groups were calculated with individual univariate ANOVAs and post-hoc Tukey Honest analyses. Statistical significance was set to $p<0.05$. PLSR was performed in MATLAB and ANOVAs and post hoc tests were computed in JMP® Pro 16.0.0.

Aim 2: Determination of Exercise Effects on OA Associated Inflammation

Intra-articular inflammation plays a critical role in mediating degradative interactions between joint tissues in OA pathogenesis. Exercise reduces systemic inflammation by controlling cytokine signaling and their associated pathways. After establishing positive tissue health effects with our exercise regimen, we then questioned how MMT surgery and exercise therapy altered the inflammation within the knee joint. Thirty-two (n = 32) male Lewis rats were acclimated to the exercise therapy and then split into the same four treatment groups (8 rats/group). Rats underwent either sham or MMT surgery. Exercise groups followed the same exercise regimen of 10 m/min for 30 min/d, 5 d/wk, 3 weeks after surgery. The study ended 6 weeks post-surgery and all animals were euthanized with CO_2 asphyxiation. Gait and tissue morphology were collected using EDGAR and EPIC micro-CT, respectively, at the same time points as in the first experiment (Figure 7).

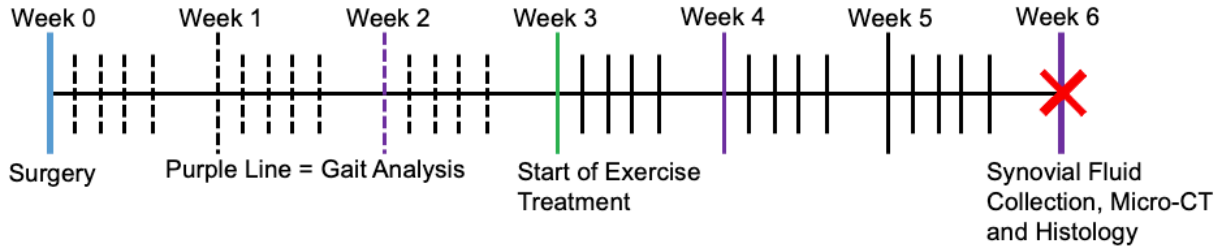

Figure 7. Timeline of Aim 2 Experiments. Surgeries were indicated as Week 0. Exercise treatment began 3 weeks (21 days) following surgery and continued for an additional 3 weeks (Solid Lines). Gait analysis was performed prior to surgery and 2-, 4- and 5-weeks following surgery (Purple Lines). Post-mortem analysis included Micro-CT, histology, and synovial fluid cytokine analysis to quantify intra-articular inflammation.

2.8 Synovial Fluid Collection

Synovial fluid was collected after animals were euthanized by inserting a Whatman filter paper into the knee joint and flexing and extending the knee. The filter paper was incubated in saline overnight. The saline solution was then centrifuged, and the supernatant was analyzed using a multiplex Enzyme-linked Immunosorbent Assay (ELISA) array. A total of twenty-seven

(n=27) inflammatory cytokines (SI 2) were measured and standardized using a multiplex ELISA kit (Milliplex Immunology Kit).

2.9 Statistical Analysis of Cytokines

Cytokine and micro-CT measurements were separately analyzed as dependent variables using the same PLSR MATLAB algorithm as the previous experiments. This reduced the multivariate spaces down to three LVs each. Univariate ANOVAs and post hoc Tukey honest tests detected differences within the tissue morphological parameters and cytokine profiles across treatment groups. Lead cytokines that best predicted overall tissue health (first LV of tissue PLSR) were identified using a step-wise linear regression that used the first LV of tissue morphology as the dependent variable. Linear regressions were conducted to analyze the associations between lead cytokines and tissue morphological parameters. Statistical significance remained at $p<0.05$.

3. Results

Aim 1: Effectiveness of the Developed Preclinical Exercise Therapy Model for OA

3.1 Literature Review for Exercise Parameter Establishment

Dosage (min/wk), Intensity (m/min), Onset (d) and Duration (wks) were collected from all twenty-five (n=25) articles obtained from the literature search. With the specified intervention time of 30 min/day for 5 days/wk, positive tissue health effects were identified with a minimum intensity of 10 m/min (Figure 8A).

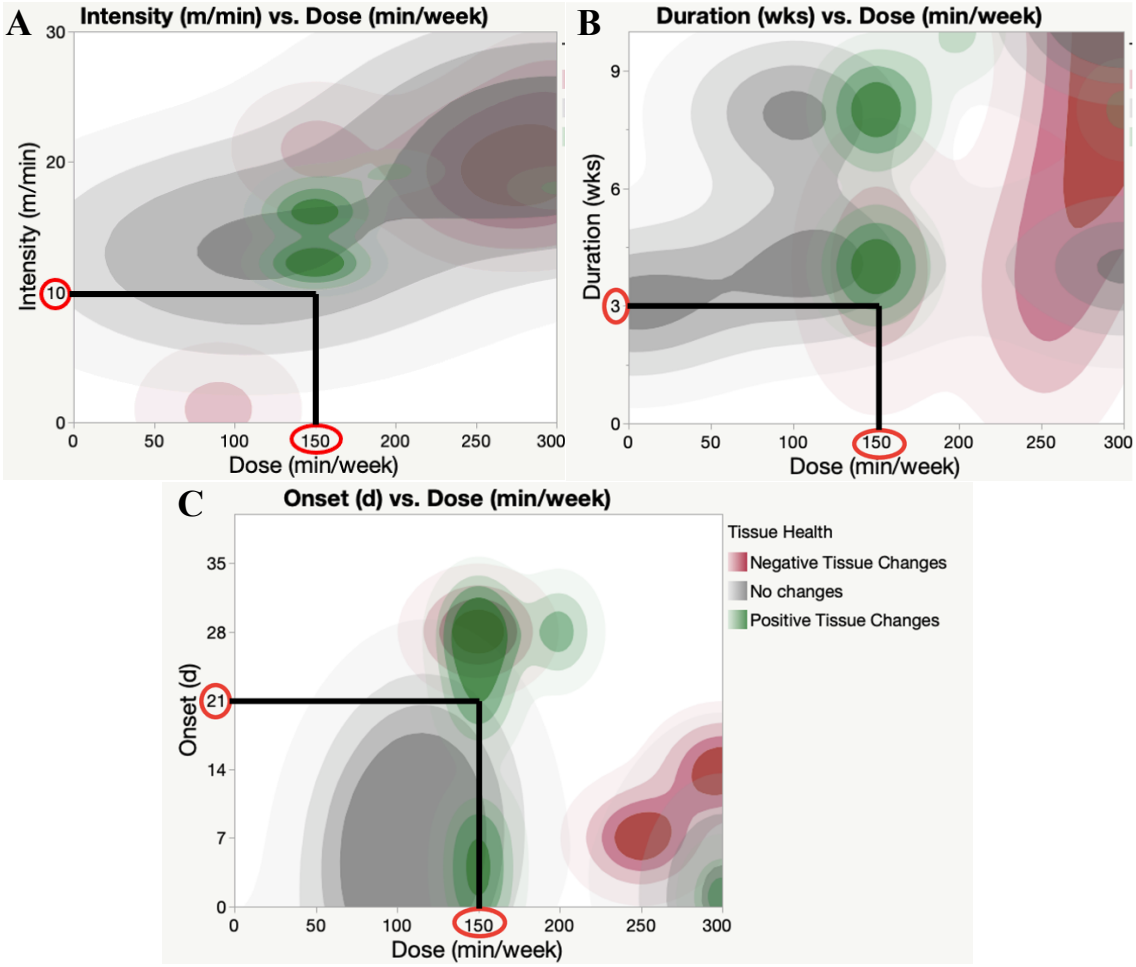

Figure 8. Determination of Intensity (A), Duration (B) and Onset (C) of Exercise based on Joint Tissue Effects and Dosage using JMP® Pro 16.0.0. The specified dosage for the exercise therapy was 150 min/week. Minimum intensity, duration and onset that were associated with positive tissue changes (green contours) were selected as the exercise therapy parameters.

Similarly, a duration of 3 weeks and an onset of exercise 21 days (3 weeks) post induction of OA were correlated with positive tissue effects when the exercise dosage was set to 150 min/wk (Figure 8B, C). Therefore, an exercise regimen of 30 min/day, 5 days/week at 10 m/min for 3 full weeks, 21 days following OA initiation was selected as the exercise treatment for our experiments.

3.2 Exercise Compliance

Ten out of the twelve exercised animals (Sham + Exercise and MMT + Exercise) exhibited 100% compliance to the established exercise therapy treatment. One rat in the MMT +

Exercise group walked an average of 26.12 min/day rather than the intended 30 min/day and was included in the study. The other non-compliant rat was in the Sham + Exercise group and averaged walking 0.12 min/day, resulting in exclusion from the study.

3.3 Joint Functional Analysis

MMT surgeries imparted negative effects on the spatiotemporal symmetry of gait six weeks post-operation. Sham animals had lower first latent variable (LV1) gait scores than the MMT group (Figure 9, p=0.01). Lower LV1 scores were indicative of greater fore step widths, more balanced hind limb spatial symmetry and lower hind step widths (SI 3). The developed exercise regimen lowered the LV1 score within MMT animals (p=0.02). The LV1 scores between the MMT + exercise group and both sham groups did not significantly differ (p=0.41 for sham and p=0.24 for sham + exercise), indicating that the prescribed exercise therapy was able to restore gait spatiotemporal symmetry.

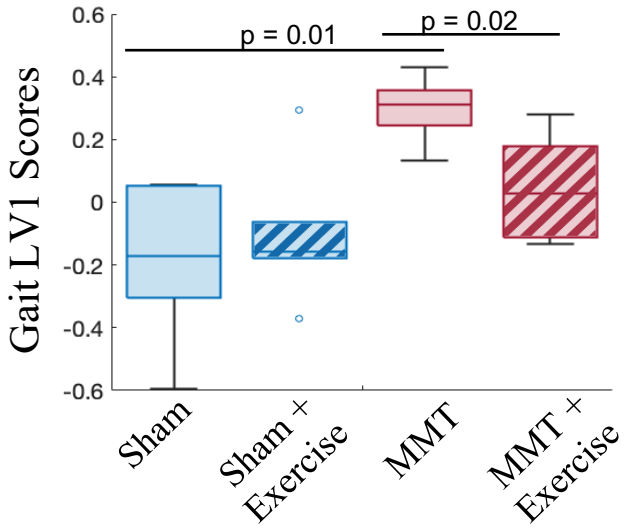

Figure 9. Functional analysis of the joint through spatiotemporal symmetry of gait using EDGAR. MMT surgeries reduced spatiotemporal symmetry as indicated by a significantly higher LV1 score in MMT animals versus Sham animals (p=0.01). Exercise was able to restore functional gait, such that the MMT + Exercise group had a significantly lower LV1 score than the MMT group (p=0.02) and was not significantly different from the sham or sham + exercise groups (p=0.41 and 0.24, respectively). Restoration of functional gait illustrates the positive effects of the exercise regimen as an OA treatment. Statistical significance was set to $p<0.05$.

3.4 Exercise Effects on Tissue Morphology

MMT surgeries resulted in the development of moderate OA in the knee joint three weeks post-operation for all MMT rats. Overall joint tissue health was reflected using a PLSR that used the morphological parameters as inputs. MMT surgery resulted in a significantly higher morphological LV1 than sham animals (Figure 10; $p<0.001$). Greater LV1 scores were indicative of increased cartilage and subchondral bone attenuation (~loss of proteoglycans and bone mineralization, respectively), osteophyte growth, and elevated cartilage surface roughness (Figure 11).

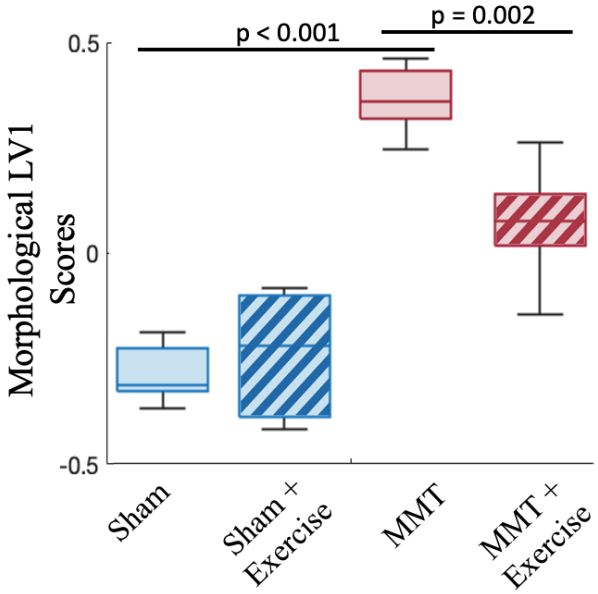

Figure 10. Morphological LV1 scores for Aim 1 Experiments using PLSR. MMT significantly increased the LV1 scores in comparison to both sham groups ($p < 0.001$), indicating a negative impact on tissue health. Exercise was able to reduce the LV1, such that there was a significant difference between the MMT and MMT + Exercise groups ($p=0.002$). This demonstrated how the established exercise regimen was able to improve overall tissue health. Statistical significance was set to $p<0.05$.

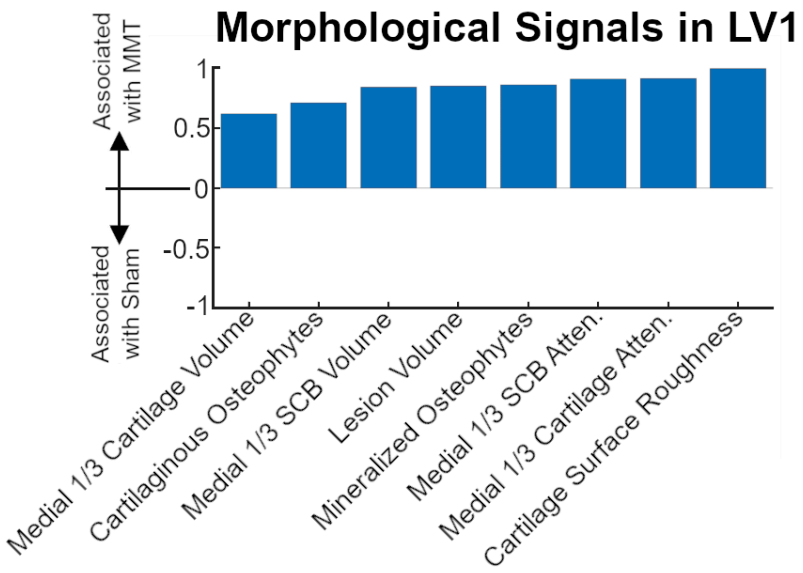

Figure 11. Morphological signals from the LV1 score of PLSR. Numerous morphological characteristics were associated with the MMT group, or the development of OA. Notably, higher LV1 scores were indicative of elevated cartilage surface roughness, cartilage attenuation (loss of proteoglycans), subchondral bone (SCB) attenuation (loss of bone mineral density) and osteophyte growth.

MMT + exercise animals had lower LV1 scores than the MMT only group (Figure 10; $p=0.002$), demonstrating how exercise reduced signs of joint degradation. However, sham and sham + exercise both had lower LV1 scores than the MMT + exercise group (sham: $p<0.001$ and sham + exercise: $p=0.002$). Univariate ANOVAs exhibit the reduction of cartilage attenuation (SI 4A; $p<0.001$), cartilage lesions (SI 4D; $p=0.036$), subchondral bone volume (SI 4E; $p=0.034$), and mineralized osteophyte sizes (SI 4C; $p<0.001$) between sham and MMT animals. Among these morphological parameters, exercise lowered cartilage attenuation (SI 4A;$p=0.027$) and cartilaginous osteophyte volumes (SI 4B; $p=0.011$) in MMT treated animals. No significant difference was observed in subchondral bone volume (SI 4E; $p=0.278$) and attenuation (SI 4A; $p=0.082$) between MMT+ exercise and sham animals, suggesting exercise's role in reducing subchondral bone remodeling. Nonetheless, this may be due to the lower values of one animal.

Aim 2: Developed Exercise Regimen Effects on OA Associated Inflammation

3.5 Tissue Morphological Changes in Aim 2

Similar to Aim 1, MMT surgeries led to the development of moderate OA for all MMT rats. This was characterized using the same PLSR technique, in which a higher LV1 score in MMT versus sham ($p<0.001$) was attributed to increased cartilage and subchondral bone volumes, subchondral bone density, and cartilage attenuation (~loss of proteoglycan) (Figure 12).

Exercise significantly reduced signs of joint degradation, such that the MMT + Exercise group also had lower morphological LV1 scores ($p=0.023$) in comparison to the MMT group. Univariate ANOVAs illustrated that MMT + Exercise animals had smaller cartilage lesions (SI 5A; $p<0.001$), reduced subchondral bone thickness (SI 5C; $p=0.027$), and smaller osteophytes (SI 5B; $p<0.001$) than the unexercised MMT animals.

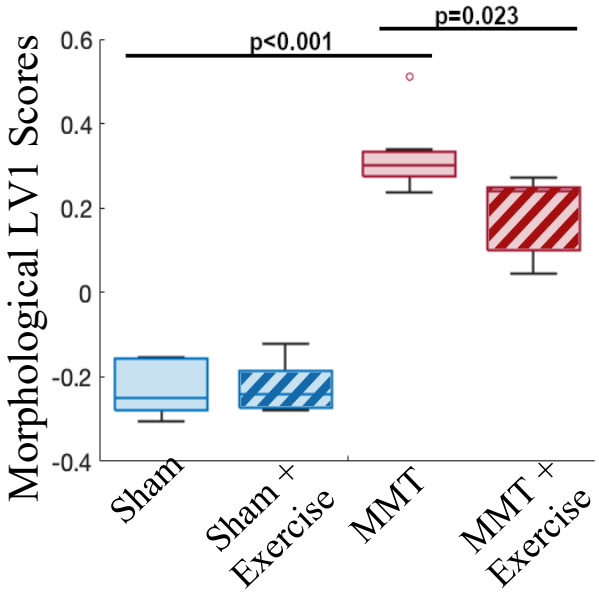

Figure 12. Morphological LV1 scores for Aim 2 Experiments using PLSR. MMT significantly increased the LV1 scores in comparison to both sham groups ($p < 0.001$), indicating a negative impact on tissue health. Exercise was able to reduce the LV1, such that there was a significant difference between the MMT and MMT + Exercise groups ($p=0.023$). This demonstrated how the established exercise regimen was able to improve overall tissue health. Statistical significance was set to $p<0.05$.

3.6 Lead Cytokine Identification

The inflammatory cytokine profiles of the synovial fluid were significantly altered at the 6-week time point following MMT surgeries. This was captured by a higher cytokine LV1 score in comparison to sham animals (Figure 13; $p<0.001$). Increased inflammation, as designated by higher LV1 cytokine scores, was associated with elevated IFN-γ and IL-10 levels and lower levels of EGF, IP-10 and VEGF (Figure 14).

The MMT + exercise group had lower cytokine LV1 scores than the MMT only group ($p=0.02$, Figure 13). No significant difference was observed between the MMT + exercise and sham groups ($p=0.77$), indicating a potential restoration of the cytokine profile because of exercise treatment.

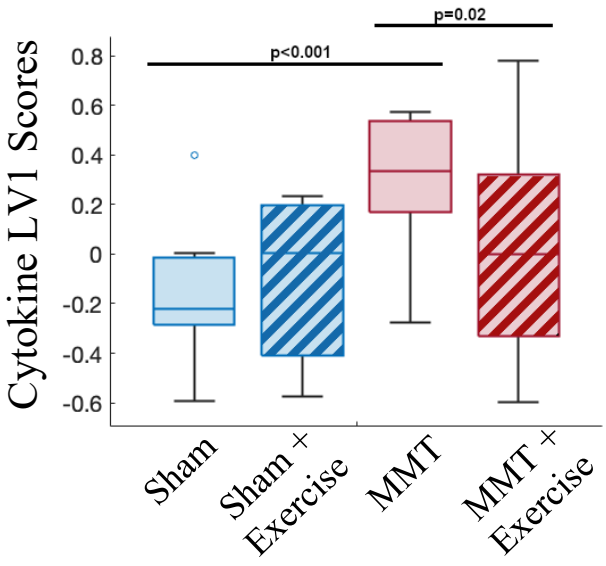

Figure 13. Cytokine LV1 scores using PLSR. MMT significantly increased the LV1 scores in comparison to both sham groups ($p < 0.001$), indicating an increase in inflammation in the synovial fluid. Exercise was able to reduce the LV1 score, such that there was a significant difference between the MMT and MMT + Exercise groups ($p=0.02$). No significant difference between the MMT + Exercise and sham group ($p=0.77$) was observed, indicating a potential restoration of synovial inflammation. Statistical significance was set to $p<0.05$.

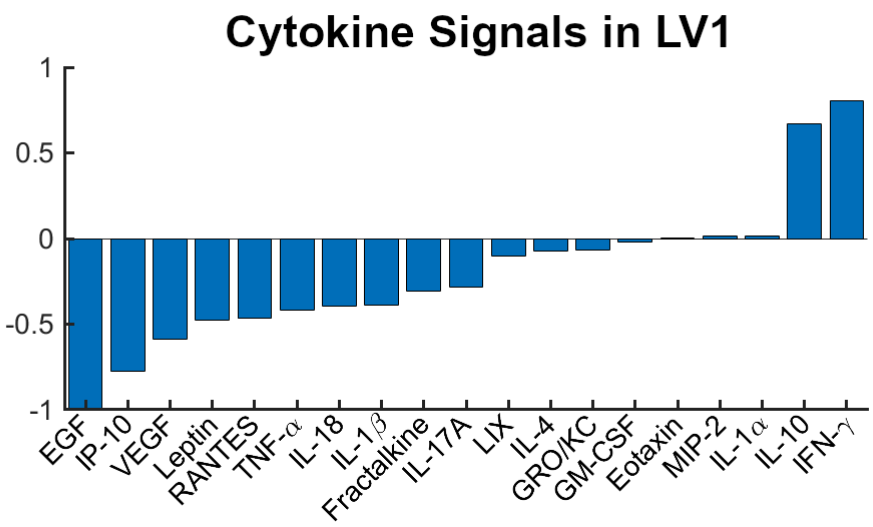

Figure 14. Stepwise linear regression using the morphological LV1 score as the dependent variable. Elevated synovial inflammation was associated with higher levels of IL-10 and IFN-γ, and lower levels of EGF, IP-10 and VEGF. IP-10 and IL-10 accounted for 44% of the variability in tissue morphology across the treatment groups, indicating a potential role of these two regulators in exercise therapy.

Among all the cytokines profiled, IP-10 and IL-10 were the best predictors of tissue health, explaining 44% of the variability of the morphological LV1 scores across all rodents (Figure 14). Elevated levels of IL-10 and lower levels of IP-10 were associated with a higher morphological LV1 score, indicating greater tissue damage with these conditions in the synovial fluid. Reduced IP-10 levels were associated with increased subchondral bone thickness (Figure 15A, R^2=0.16, p=0.037) and subchondral bone attenuation (Figure 15B, R^2=0.22, proportional to mineralization; p=0.013). These morphological changes were indicative of subchondral bone sclerosis, or the increase in the density of bone. Higher levels of IL-10 were associated with greater mineralized osteophyte volumes (Figure 15C, R^2=0.15, p=0.039) and more exposed bone, or the greater loss of articular cartilage (Figure 15D, R^2=0.25, p=0.007). Hence, lower levels of IL-10 and higher levels of IP-10 were associated with the reduction of OA pathogenesis.

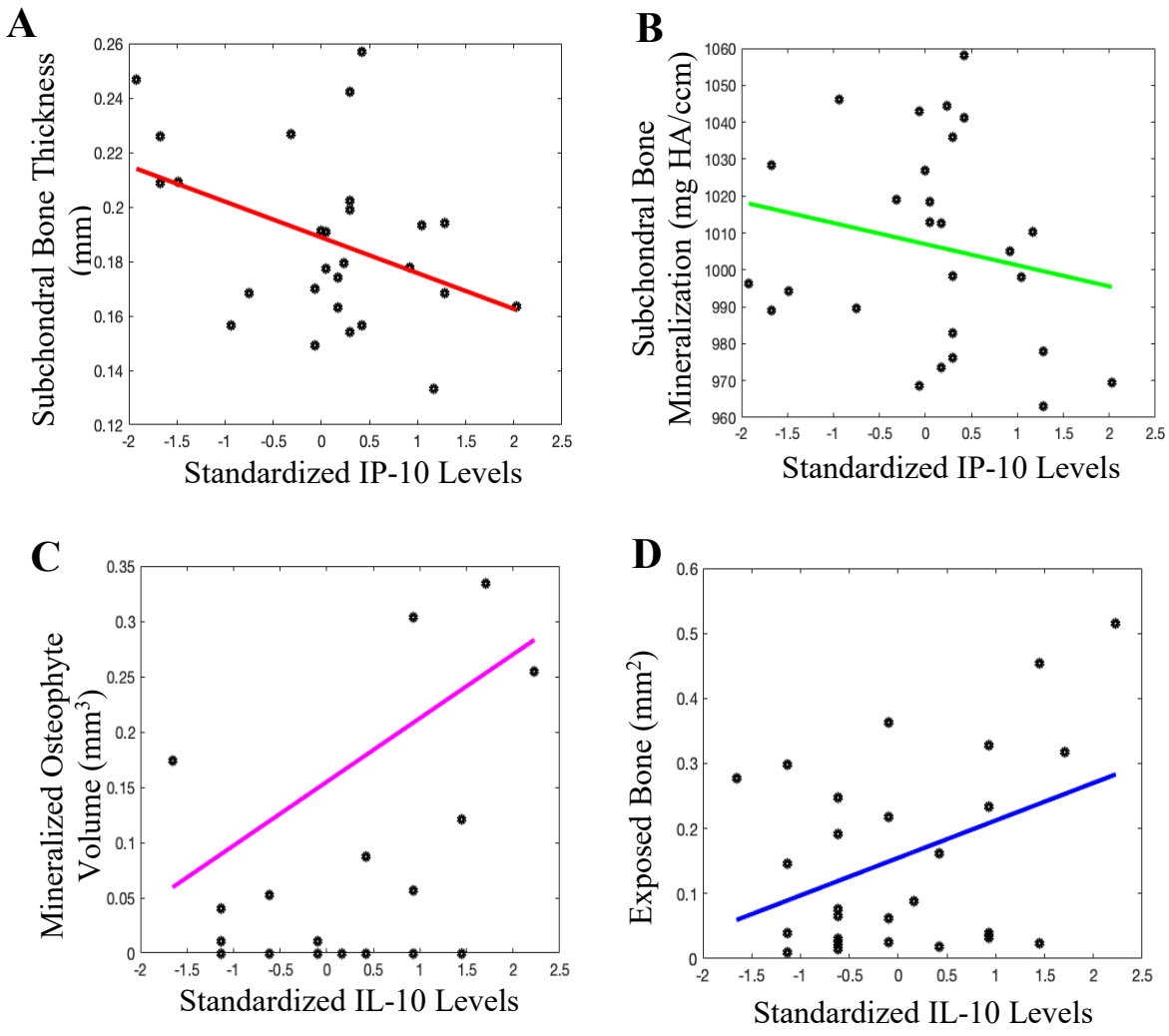

Figure 15. Linear regression analysis of IP-10 and IL-10 and their associated tissue morphological parameters. IP-10 was negatively correlated with subchondral bone thickness (A, R^2=0.16, p=0.037) and subchondral bone mineralization (B, R^2=0.22, p=0.013). This was indicative of a possible anti-sclerotic response generated by IP-10. IL-10 was positively correlated with mineralized osteophyte growth (C, R^2=0.15, p=0.039) and increased exposed bone, or cartilage degradation (D, R^2=0.25, p=0.007). Thus, specific morphological changes in the joint tissue were associated with IP-10 and IL-10 levels, indicating exercise's role in regulating these two signaling molecules in reducing OA pathogenesis. Statistical significance was set to $p<0.05$.

4. Discussion

Exercise therapy is one of the only successful treatments found to reduce osteoarthritic pain and slow disease progression. Although exercise is the "gold-standard" of OA treatment, there are two caveats that limit its widespread applicability. The first issue arises from variations in exercise treatment parameters, which lead to differential outcomes on tissue health and pain. The second problem is the lack of patient adherence, such that the long-term benefits of exercise are often not fully realized.[48] As a result of both issues, exercise's therapeutic effects against OA are generally misunderstood. In this thesis, we sought to address both caveats by standardizing a beneficial exercise regimen in a pre-clinical model. We then used this model to study the biochemical inflammatory pathways in which exercise reduces OA pathogenesis. This was done to identify a potential pharmaceutical target (i.e. "exercise injection") that could be used to elicit the same positive response of exercise to overcome the issue of patient non-compliance.

In determining the parameters for our developed exercise regimen, we considered the multitude of factors that determine the therapeutic capacity of a prescribed exercise therapy. Among these, variation in the duration, intensity, dosage and onset of exercise programs across studies make it difficult to quantify exercise's morphological and inflammatory effects on the joint. Consequently, previous studies indicate great variation in the pre-clinical outcomes of exercise treatment, demonstrating both detrimental and therapeutic effects on joint tissue health. For example, two days following joint destabilization, short, frequent and moderately intense treadmill walking sessions over a 6 week period reduced subchondral bone growth, osteoclast development and cartilage degeneration in a preclinical rodent model.[50] Conversely, strenuous running for longer time intervals over 3 weeks exacerbated cartilage erosion in rats.[51] Hence, standardizing an exercise regimen that exhibits therapeutic effects on joint tissues was first

needed before we could elucidate any inflammatory pathways associated with the benefits of exercise on joint preservation.

In this study, we performed a literature search to establish a pre-clinical rodent exercise therapy that elicited chondroprotective effects. Based on this literature search, we used mild treadmill walking for 30 min/day, 5 days/week at 10 m/min for 3 full weeks, 21 days following OA initiation. Through this exercise program, we observed beneficial tissue effects, including reduced subchondral bone remodeling, limited osteophyte growth, and the minimization of articular cartilage loss (SI 4). Exercise also decreased the LV1 morphological and gait scores in comparison to non-exercised OA animals, demonstrating our exercise regimen's ability to improve overall tissue health and spatiotemporal symmetry of gait (Figure 9 and Figure 10). Based on these positive findings, we utilized this exercise protocol to identify how synovial inflammation is associated with therapeutic exercise since tissue morphological changes are exacerbated by inflammation.[17]

Synovitis describes the inflammation of the synovium, which has been found to correspond to pain throughout OA progression.[52] During both the onset and exacerbation of synovitis, the activity of both the FLS and MLS are dysregulated, resulting in the elevated secretion of inflammatory cytokines into the synovial fluid.[53] Particularly, macrophage activity, including MLS, is highly upregulated in OA, such that it greatly contributes to the increased intra-articular inflammation.[54] Similarly, activated MLS stimulate other immune cells, recruiting T cells and other macrophages to the joint to promote inflammation in the intra-articular environment.[55] Through this elevated inflammation, the cytokines secreted by dysregulated MLS contribute to joint degradative changes, including subchondral bone remodeling, osteophyte

formation and cartilage degradation, by interacting with the cellular and protein components of the other tissues within the joint.[56,57]

Subchondral bone remodeling is initiated by the formation of bone marrow lesions, which are associated with the mechanical overloading of the joint.[22] Bone marrow lesions develop in the early stages of OA progression, simultaneously with the onset of synovitis, and before any radiographic changes to the joint are observed.[58] Bone marrow lesions lead to the reparative development of blood vessels and increased inflammation. This is observed alongside of the improper healing of micro-fractures of the bone plate. These events lead to the propagation of subchondral bone remodeling.[59, 60] Subsequently, the early stages of subchondral bone remodeling result in bone resorption, whereas in the later stages of OA, excessive bone formation occurs.[61]

Due to the early coexistence of synovitis and subchondral bone remodeling, synovitis and its associated immune cell recruitment may play a critical role in the exacerbation of subchondral bone remodeling.[57] Macrophage activation, including MLS, can lead to the over production of TNF-α and IL-1, triggering the dysregulation of osteoblast, osteoclast and osteocyte activity.[62,63] MLS also have the capability to differentiate into osteoclasts upregulating osteoclastogenesis, or bone resorption.[64, 65] Thus, synovial inflammation, specifically through the activity and regulation of macrophages, plays an important role in mediating subchondral bone resorption and formation.

Osteophytes are derived from the proliferation and differentiation of MSC on the periosteum, localized to the margins of the cartilage.[66] Proliferation of these MSC are associated with synovial inflammation. More precisely, MLS secrete pro-inflammatory cytokines and bone-generating growth factors, such as BMPs, which can then catalyze the formation of

osteophytes.[67] During osteophyte formation, MSC first undergo chondrogenesis to produce cartilaginous outgrowths. Through the hypertrophy and enchondral ossification of these derived chondrocytes, the cartilaginous osteophytes transform into mineralized osteophytes.[64] Hence, synovial inflammation, particularly MLS activity, help accelerate osteophyte formation through the secretion of pro-inflammatory cytokines and growth factors that aid in the proliferation of the MSC on the periosteum.

Intra-articular inflammatory signaling amplifies the loss of articular cartilage through the crosstalk between chondrocytes and synoviocytes. One of the key cyclical pathways that promotes both synovitis and cartilage degeneration is the binding of cartilage ECM fragments to synoviocytes, prominently MLS, leading to the downstream activation of the NF-kB pathway.[27,28] This results in the elevated secretion of TNF-α and IL-1β into the synovial fluid. These cytokines then bind to chondrocytes in the cartilage ECM, triggering the production of MMP-3 and MMP-13, whose proteolytic activity further breaks down cartilage ECM components.[21] Based on this primary pathway in OA progression, MLS play an important role in furthering the breakdown of cartilage, such that the depletion of MLS from osteoarthritic synovium lowered the expression of MMPs.[68]

Overall, synovial inflammatory regulation within the intra-articular space, especially by macrophages, plays a key component in the onset and progression of OA through all three joint tissue degradative changes. Through this, we sought to identify how our exercise regimen impacted the synovial fluid inflammatory profile and how differential cytokine signaling pathways may be associated with specific joint morphological results. Our developed exercise treatment reduced intra-articular inflammation in our preclinical model, as illustrated by the lower LV1 cytokine scores for the exercised OA group in comparison to the non-exercised OA

group (Figure 13). In this study, we found that IL-10 and IP-10 accounted for 44% of the variability of joint morphological changes between the exercised OA group and the non-exercised OA group (Figure 14). Standardized IL-10 levels were positively correlated with increased areas of exposed bone, or excessive cartilage loss, and greater osteophyte volumes (Figure 15C and D). IP-10 was negatively associated with subchondral bone mineralization and volume, suggesting that exercise increased IP-10 levels, leading to reduced subchondral bone sclerosis (Figure 15A and B). Due to their key roles in regulating inflammation in the joint space, the complex activity of macrophages may explain these shifts in IL-10 and IP-10 levels with respect to both OA progression and exercise treatment.

Macrophages are immune cells whose jobs are to phagocytose cellular debris at the sites of infection. The activity of macrophages is dictated by the cell's phenotype, in which cells can be broadly categorized as either "pro-inflammatory", termed M1 macrophages, or "immunoregulatory" also known as M2 macrophages (Figure 16A).[69,] Categorization of these cells is dependent on the stimulus of cellular activation and their associated cytokine secretory response. In general, monocytes, or macrophage predecessors, polarize toward the M1 phenotype by binding to either interferon gamma (IFN-γ) or lipopolysaccharide (LPS). This results in the secretion of TNF-α and IL-1 in addition to a variety of other "pro-inflammatory" cytokines. In contrast, M2 activation occurs as a result of binding to "anti-inflammatory" cytokines, including IL-10. Such stimulation leads to the secretion of more IL-10 but also the IL-1 receptor agonist.[70]

Classifying M2 macrophages, however, can be broken down even further into three types: M2a, M2b and M2c. Interestingly, M2b macrophages are considered "regulatory macrophages" because they can be activated by the binding of LPS, like M1 macrophages. M2b activity results in the secretion of IL-10, similar to its M2 classification, but also produces

excessive amounts of TNF-α and IL-1β comparable to M1.[71] Previous screening of MLS phenotypes in OA has identified a combination of M1 and M2 markers, indicating a mixed expression of M1 and M2 phenotypes in the synovium.[72,73] Since M2b macrophage activity exhibits characteristics of both M1 and M2, MLS polarization towards an M2b phenotype may occur during the development of OA.

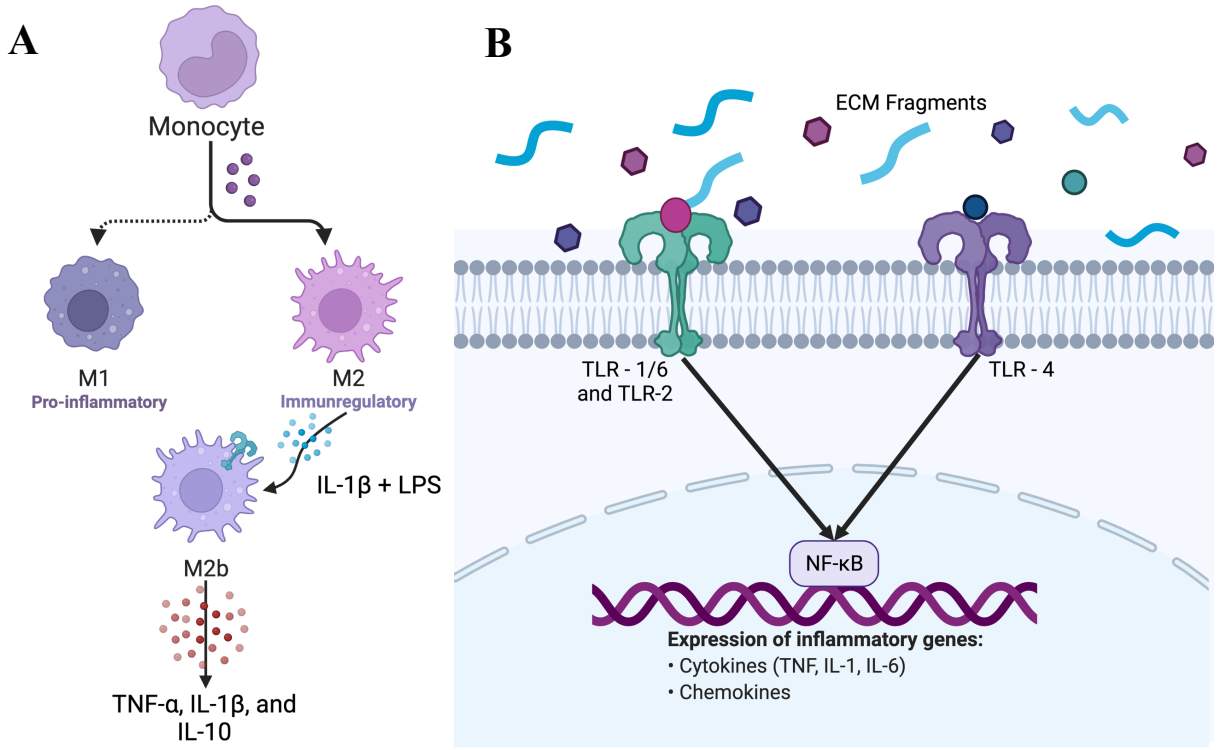

Figure 16. (A) Macrophages are immune cells that phagocytose cellular debris at areas of infection. Characterization of macrophages can be broadly split between M1 (pro-inflammatory) and M2 (immunoregulatory). M2 macrophages can also adopt sub-phenotypes, such as M2b, which are stimulated by and secrete cytokines of the M1 phenotype. **(B)** Toll-like receptors (TLRs) are membrane bound proteins that reside on immune cells. Stimulation of TLRs leads to the activation of the NF-kB pathway, triggering a pro-inflammatory response. TLR-2 forms a heterodimer with TLR-1 or TLR-6 when active. TLR-4 is often stimulated by LPS. ECM fragments can also bind to these proteins, leading to their enhanced activity. (Made on Biorender).

In particular, the activation of M1 and M2b can be stimulated by the binding of LPS to the cell membrane. LPS is a toll-like receptor ligand, such that LPS binds to a specific protein on the macrophage called a toll-like receptor (TLRs). TLRs are membrane bound proteins that play a key role in immune system responses through their recognition and activation by microbial-derived molecules (Figure 16B). After binding to their specific microbial targets, TLRs activate

the pro-inflammatory NF-kB pathway, leading to the secretion of TNF-α and IL-1β.[74] Nonetheless, stimulation of TLRs on M2b macrophages also result in the production of IL-10.[70] This may explain why IL-10 was positively associated with both osteophyte growth and greater exposed bone volumes in our OA groups.

TLR-4 and TLR-2 are the two TLRs that are most prominently found to play a role in OA development.[75] Among many other molecules, TLR-4 most notably recognizes and binds to LPS, generating its associated inflammatory response.[76] TLR-2, on the other hand, forms a heterodimer with either TLR-1 or TLR-6, such that it can be activated by a large variety of stimuli.[77] Expression of TLR-4 and TLR-2 are increased in cartilage lesions and inflamed synovia in osteoarthritic knees. This is due to damage-associated molecular patterns (DAMPs), such that broken ECM fragments from degraded cartilage can bind to TLR-4 and TLR-2 on macrophages.[78,79] To this extent, TLR-4 and TLR-2 activity may play a key role in OA pathogenesis by activating M2b associated pathways in MLS. This would include the increased secretion of TNF-α, IL-1β and IL-10. This response may contribute to our observed degradation of cartilage and osteophyte formation because elevated TNF-α, IL-1β and IL-10 in the synovial fluid can bind to chondrocytes in the ECM and MSC on the periosteum. Such cytokine signaling would trigger MMP production and osteophyte generation, respectively (Figure 17).

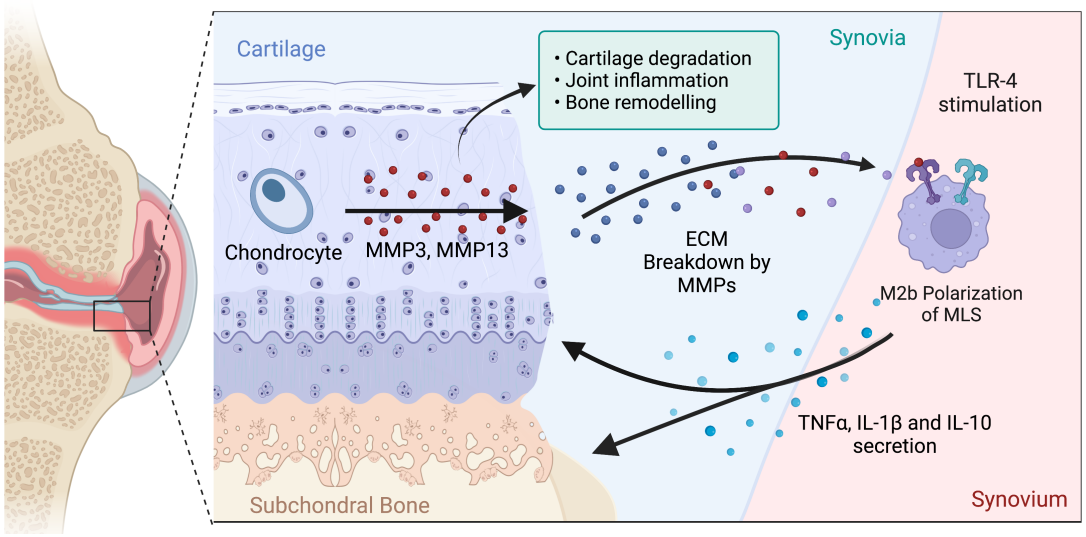

Figure 17. Proposed mechanism by TLRs on MLS for OA cartilage degradation and osteophyte formation. TLR stimulation on MLS membranes may lead to the polarization towards an M2b phenotype. This would result in the activation of the NF-kB pathway and consequent secretion of TNF-α, IL-1β and IL-10. Upregulation of these signaling molecules may explain the greater levels of exposed bone (cartilage degradation) and osteophyte formation in our OA models. (Made on Biorender).

TLR-4 and TLR-2 activity on both MLS and osteoblasts may also play a significant role in the advancement of subchondral bone remodeling through IP-10 signaling. In this thesis, IP-10 levels were negatively correlated with subchondral bone thickening and mineralization, proposing a possible anti-sclerotic response with higher IP-10 levels (Figure 15C and D). IP-10 is a chemokine that recruits T helper cells, macrophages and neutrophils to areas of infection, thereby eradicating pathogens through inflammatory responses.[80, 81] IP-10 can also initiate synovitis by signaling for the accumulation of these immune cells into the synovial membrane in both OA as well as in rheumatoid arthritis.[82] Furthermore, IP-10 promotes osteoclastogenesis by modulating cellular communication between osteoblasts and osteoclasts.[83] Therefore, enhanced expression of IP-10 is able to signal for advanced bone destruction in inflamed arthritic joints.[84,85]

TLR-2 can mediate osteoclastogenesis through its activity on osteoblasts. Following elevated bone formation by osteoblasts, stimulation of TLR-2 on osteoblast membranes aids in the regulation of bone volume (Figure 18). To elaborate, TLR-2 activation leads to the

production of IP-10 by osteoblasts. In turn, secreted IP-10 stimulates osteoclasts, resulting in an osteoclastogenic response. This stimulatory pathway results in the elevated activity of osteoclasts and thus increased bone resorption.[86,87,88] Another potential pathway activator of subchondral bone remodeling is the differentiation of MLS into osteoclasts. TLR-2 and TLR-4 activation on MLS can potentially trigger this differential response, furthering osteoclastogenic activity. Hence, between these two responses, TLR activation and its associated IP-10 signaling may explain our observed changes in IP-10 levels and the observed anti-sclerotic response.

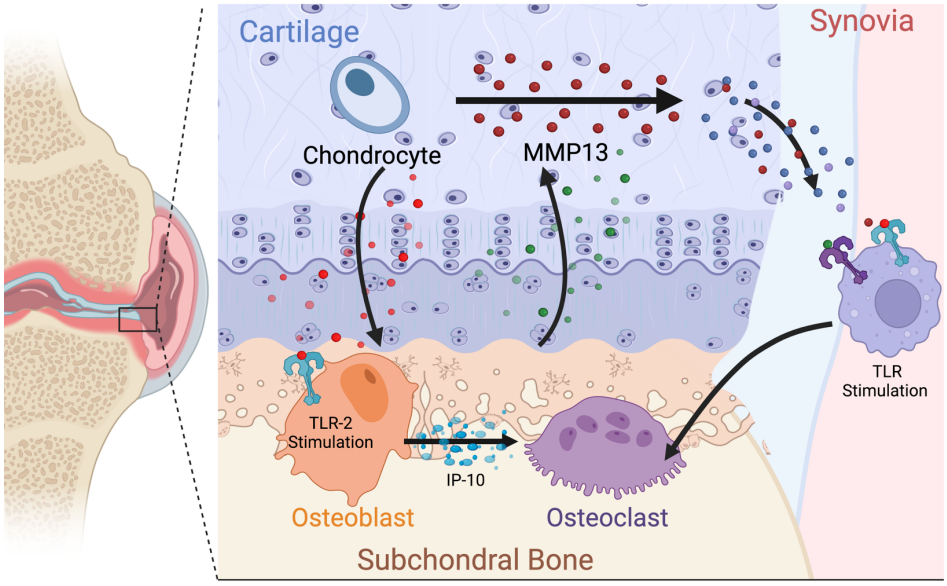

Figure 18. Proposed mechanism for IP-10 Signaling of TLRs resulting in the regulation of subchondral bone remodeling. TLR-2 stimulation on osteoblast membranes lead to the secretion of IP-10. IP-10 activates osteoclasts, promoting an anti-sclerotic response. MLS can also differentiate into osteoclasts, promoting osteoclastogenesis. (Made on Biorender).

Regulation of TLR-4 and TLR-2 are also affected by exercise as moderate levels of exercise can reduce TLR expression and systemic inflammation.[89,90] Aerobic exercise can induce a phenotypic switch in macrophages, resulting in the downregulation of TLR-4 and TLR-2 expression and their associated activation of the NF-kB pathway.[91] Based on the regulatory roles of TLRs, decreased expression of TLR-2 and TLR-4 due to exercise could explain why IL-10 and IP-10 were associated with greater areas of exposed bone, higher osteophyte volumes and

enhanced subchondral bone resorption. I suggest that our established exercise regimen may inhibit TLR activation on the MLS membrane, preventing the polarization of MLS towards an M2b phenotype (Figure 19). This would reduce circulating levels of IL-10, TNF-α and IL-1β in the synovial fluid and the subsequent activation of MMP production by chondrocytes and MSC differentiation on the periosteum. The exercise program in this study may also control IP-10 activity in the subchondral bone space, modulating TLR-2, osteoblast, and osteoclast activity (Figure 20). Further experiments identifying the roles of TLR-2 and TLR-4 in exercised OA models is needed. This may include performing exercise studies in the absence of TLR-4 and TLR-2.

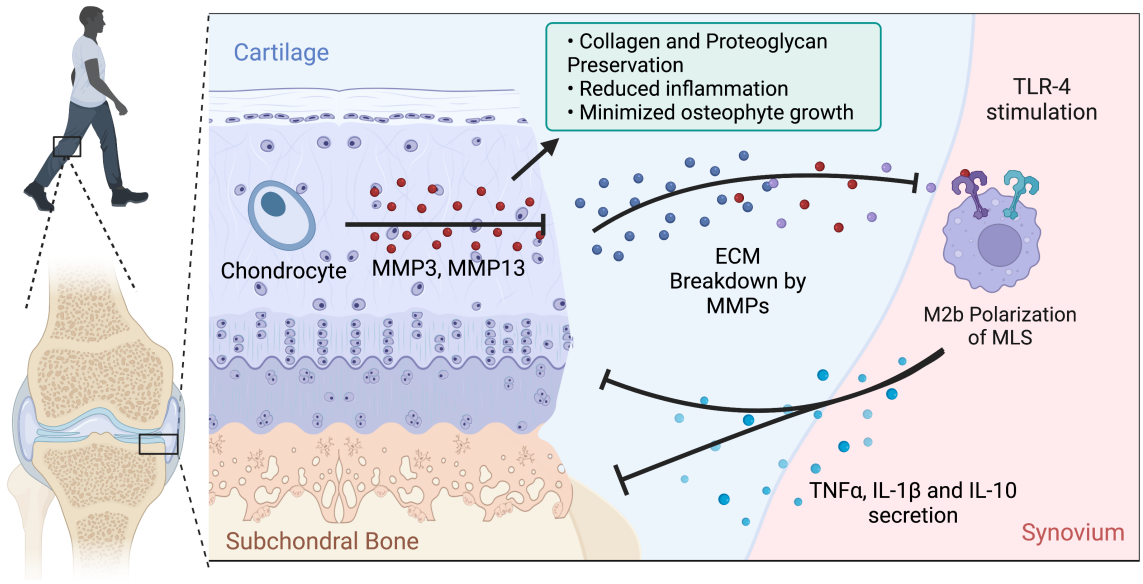

Figure 19. Proposed role of exercise in modulating cartilage degradation and osteophyte formation. Exercise may reduce TLR expression on MLS membranes, downregulating the activity of the NF-kB pathway. This would reduce IL-10, TNF-α and IL-1β levels in the synovial fluid and thus the activity of MMPs and proliferation of MSC on the periosteum. Consequently, this would reduce cartilage ECM breakdown and osteophyte formation. (Made on Biorender).

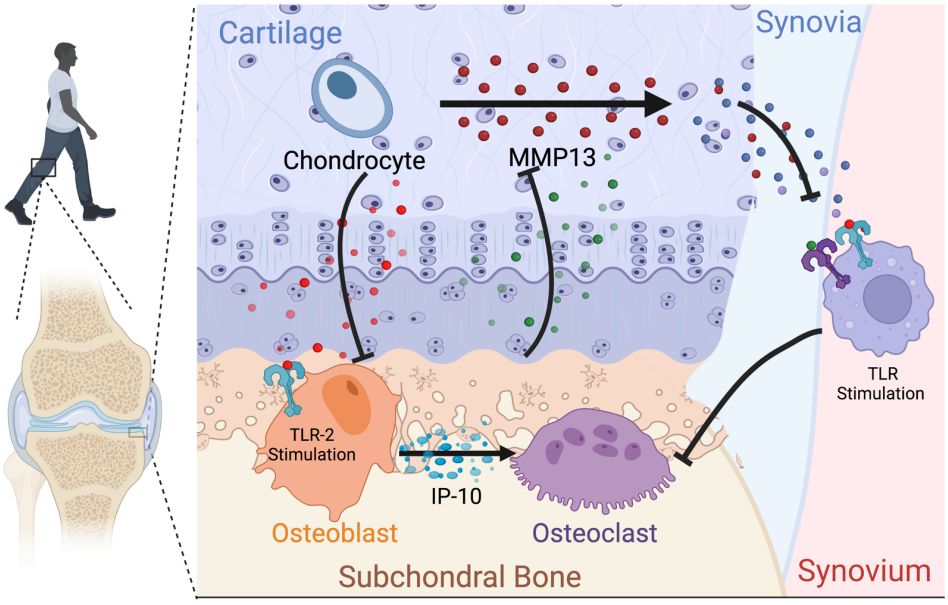

Figure 20. Proposed role of exercise on reducing subchondral bone thickening and mineralization. Exercise may regulate the expression of TLRs on osteoblasts and MLS. This would control the levels of osteoblast-secreted IP-10 and therefore the stimulation of osteoclasts. Regulation of TLR activity on MLS may also moderate MLS differentiation into osteoclasts. (Made on Biorender).

The experiments performed in this thesis were not without limitations. In this study, synovial fluid cytokine levels were only analyzed at the postmortem time point. No initial cytokine profiles were identified, such that we did not longitudinally compare the effects of exercise and OA induction on synovial inflammation. Future studies should be performed to collect synovial fluid and joint tissue morphological data at three separate time points: prior to OA induction, before the onset of exercise treatment and after the exercise program is complete. Additional experiments can be performed to improve how we determine the exercise dosage for our preclinical exercise therapy. In this study, we used twenty-five articles (n=25) to determine how intensity, duration and onset of our exercise therapy could generate positive joint health changes in our pre-clinical model. Future work should be conducted to expand our data collection and improve our analysis of these parameters. This may include conducting our own experiments, in which we vary dosage parameters. Machine learning can also be utilized to develop a data-driven model based on our expanded standardized data set. One possible machine

learning technique may include the application of Support Vector Machine (SVM) to develop a function that can best classify the data based on joint tissue health.

In conclusion, this thesis developed a preclinical exercise model that uses a mild walking exercise regimen to ameliorate the joint morphological changes and intra-articular inflammation of OA. We identified IL-10 and IP-10 as lead cytokines in explaining the variability of joint tissue health between exercised and non-exercised OA animals. Overall, controlling inflammatory mediated pathways associated with exercise therapy, such as TLR-2 and TLR-4 expression, can be a potential target to overcome the lack of patient adherence associated with exercise therapy through the development of a pharmaceutical intervention (i.e. “exercise injection”).

5. Supplementary Information

Abbreviation List:

MLS = Macrophage-Like Synoviocytes

FLS = Fibroblast-Like Synoviocytes

ECM = Extracellular Matrix

OA = Osteoarthritis

MMPs = Matrix Metalloproteinases

TNF-α = Tumor Necrosis Factor Alpha

IL-1β = Interleukin 1 Beta

MSC = Mesenchymal Stem Cells

NF-kB = Nuclear factor kappa B

BMPs = Bone Morphogenetic Proteins

IL-6 = Interleukin 6

VAMC = Veteran Affairs Medical Center

IACUC = Institutional Animal Care and Use Committee

MMT = Medial Meniscal Transection

MCLs = Medial Collateral Ligaments

EDGAR = Experimental Dynamic Gait Arena for Rodents

EPIC = Equilibrium partitioning of an ionic contrast agent

GAGs = Glycosaminoglycans

PLSR = Partial least squares regression

IL-10 = Interleukin 10

IP-10 = Interferon gamma-induced protein 10

LV = Latent variable

ELISA = Enzyme-linked Immunosorbent Assay

SCB = Subchondral Bone

IFN-γ = Interferon gamma

LPS = Lipopolysaccharide

TLR = Toll-like Receptor

DAMP = Damage Associated Molecular Pattern

SVM = Support Vector Machine

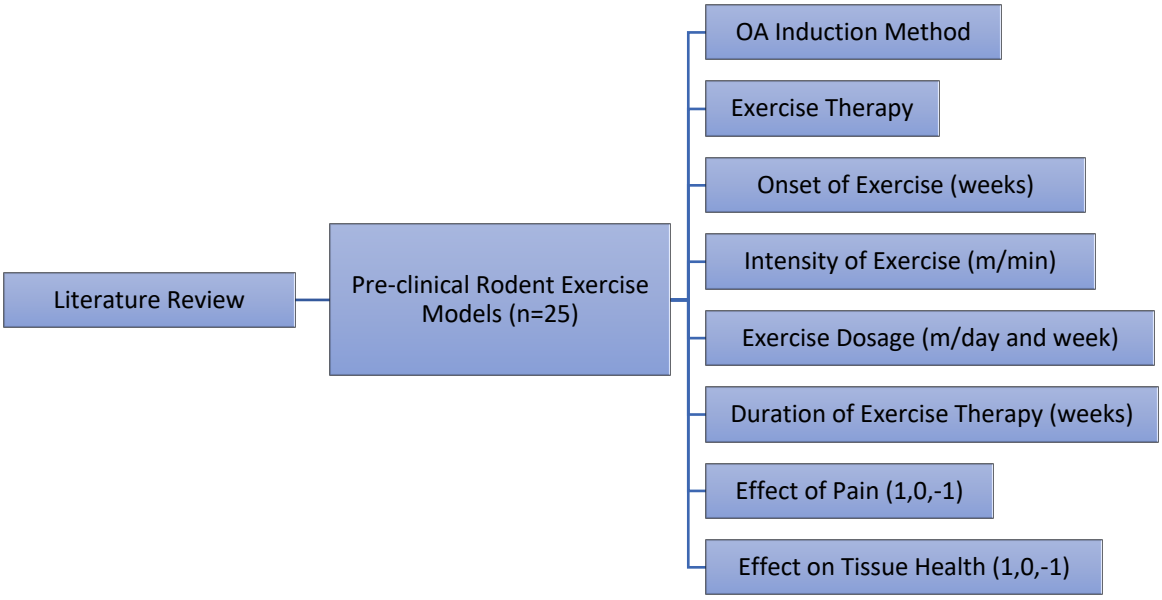

SI 1. Schematic of the literature search conducted to determine the parameters for our established exercise regimen. OA induction methods included surgeries or biochemical injections. Exercise therapy types involved wheel running, treadmill walking or incline running. The onset of exercise was referred to as when exercise sessions first began, including both prior and/or after OA induction. The intensity of exercise was the speed at which the animals were exercised. The duration of exercise therapy was how long the regimen lasted for. Pain was evaluated using multiple analysis types, including von Frey testing and thermal hypersensitivity. Tissue health was determined using multiple tests, such as micro-CT and histological staining. Scores for pain and tissue health were given as -1 for a negative change, 0 for no change and +1 for an improvement.

Cytokines (n = 19)			
Eotaxin	IP-10	IFNγ	IL-10
GM-CSF	GRO/KC	IL-17A	MIP-2
IL-1α	VEGF	IL-18	RANTES
IL-1β	TNFα	IL-4	EGF
Leptin	Fractalkine	LIX	

SI 2. List of the cytokines collected and analyzed in Aim 2's experiments. Cytokines were quantified using an ELISA multiplex array after synovial fluid was incubated and centrifuged.

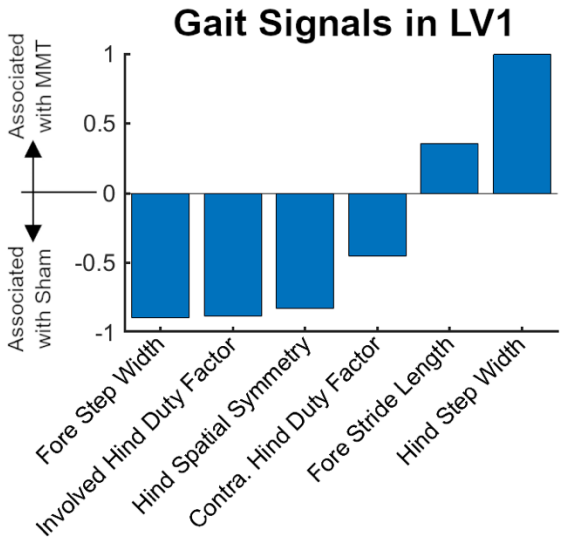

SI 3. Gait signals from the LV1 score of the PLSR. Various gait parameters were associated with the MMT group, or the development of OA, resulting in higher LV1 scores. Lower LV1 scores were indicative of greater fore step widths, more balanced hind limb spatial symmetry and lower hind step widths

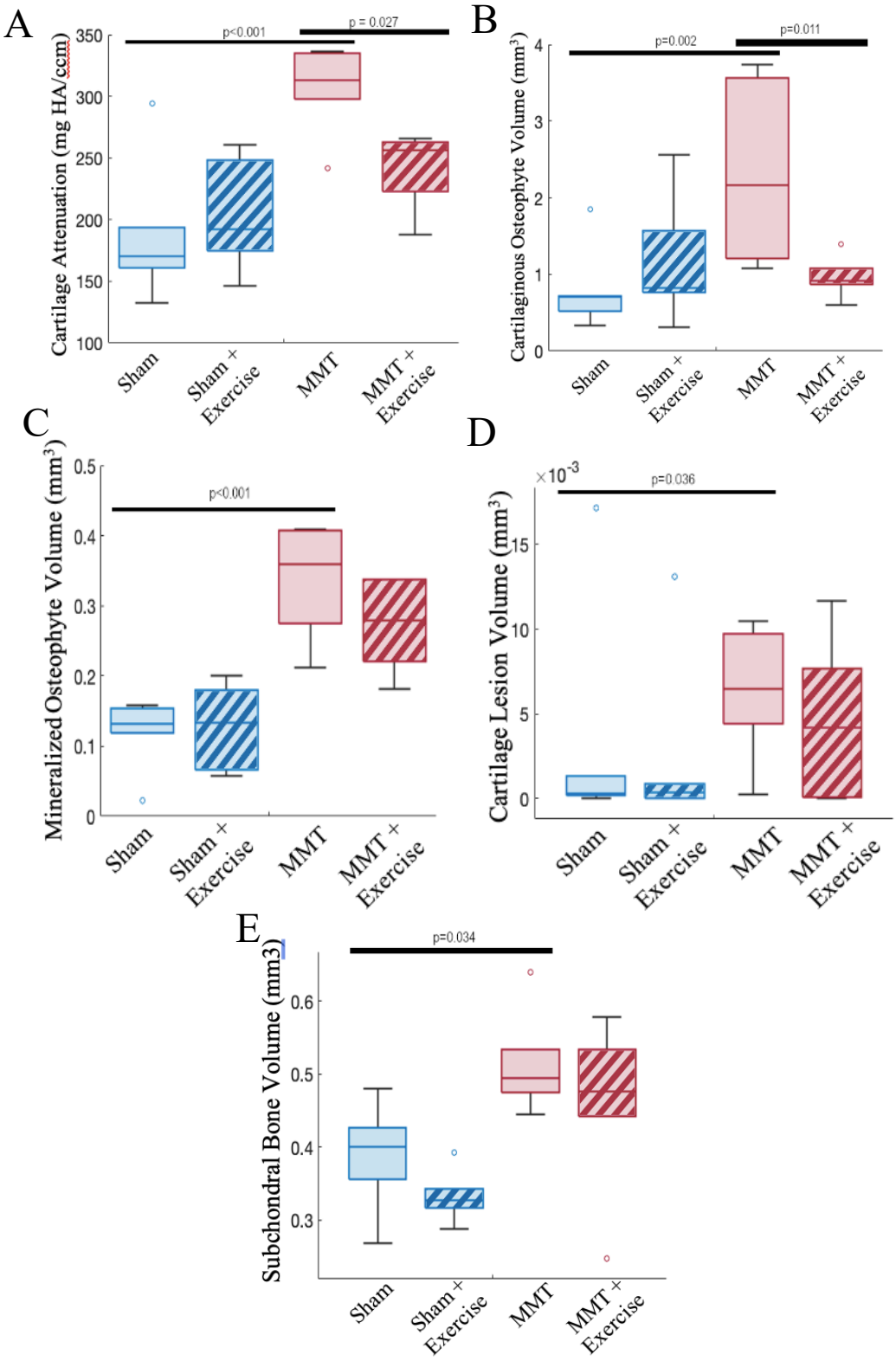

SI 4. Univariate ANOVAs and post-hoc Tukey Honest analyses for individual morphological parameters with respect to treatment groups for Aim 1 experiments. OA induction significantly increased cartilage attenuation (~loss of proteoglycans) (A; $p<0.001$), cartilaginous (B; $p=0.002$) and mineralized (C; $p<0.001$) osteophyte volumes, cartilage lesions (D; $p=0.036$) and subchondral bone volumes (E; $p=0.034$) in comparison to the sham groups.

Exercise reduced cartilage attenuation (A; p=0.027) and cartilaginous osteophyte volumes (B; p=0.011), as demonstrated by significant differences between the MMT and MMT + Exercise groups. Statistical significance was set to p<0.05.

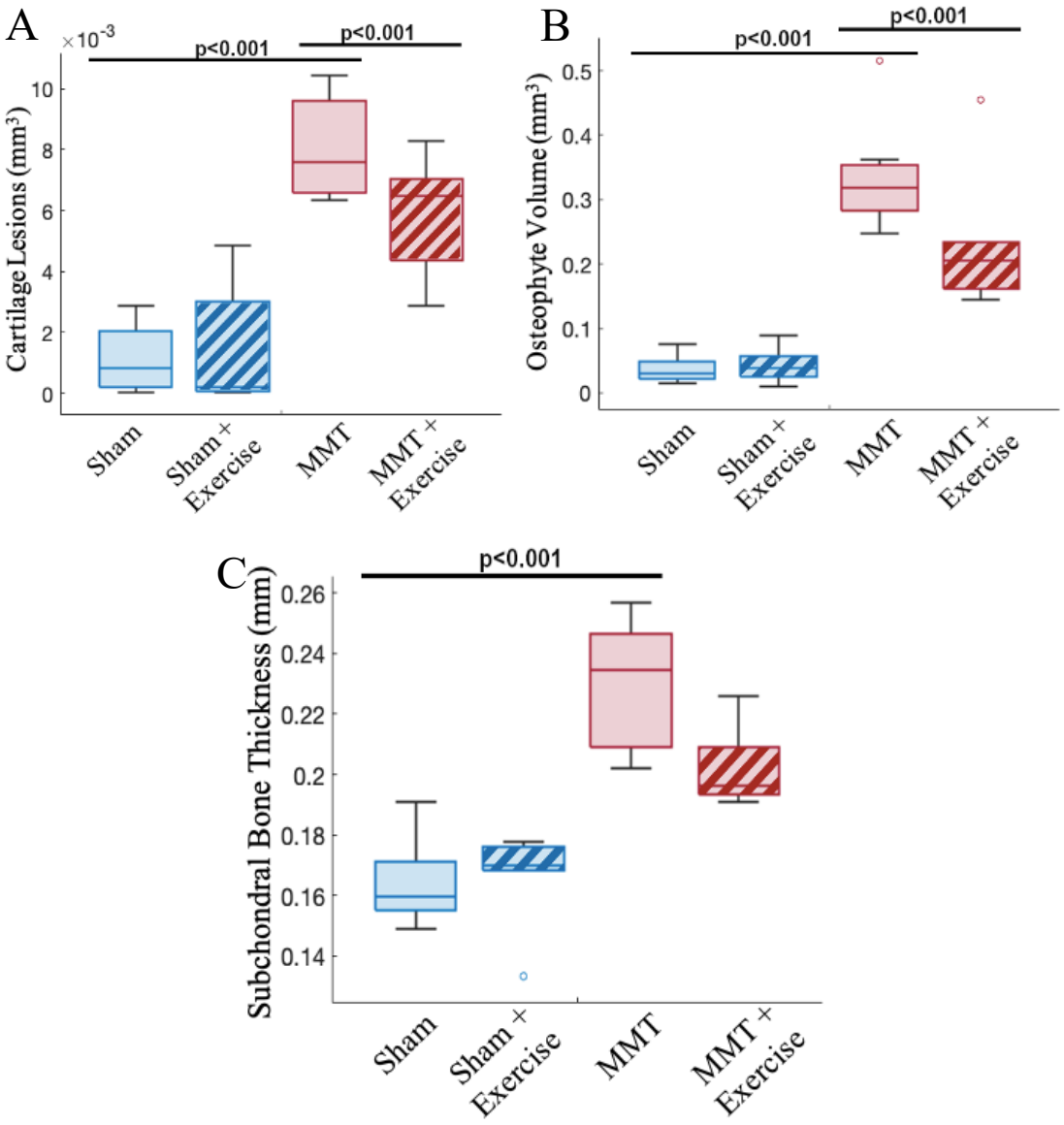

SI 5. Univariate ANOVAs and post-hoc Tukey Honest analyses for individual morphological parameters with respect to treatment groups for Aim 2 experiments. OA induction significantly increased cartilage lesions (A; p<0.001), osteophyte volumes (B; p<0.001) and subchondral bone thickness (C; p<0.001) in comparison to the sham groups. Exercise reduced cartilage lesion volumes (A; p<0.001) and osteophyte volumes (B; p<0.001), as demonstrated by significant differences between the MMT and MMT + Exercise groups. Statistical significance was set to p<0.05.

6. References

1. Anatomy of the Knee. https://www.arthritis.org/health-wellness/about-arthritis/where-it-hurts/anatomy-of-the-knee (accessed March 10, 2022).

2. Tamer, T. M. Hyaluronan and synovial joint: function, distribution and healing. *Interdiscip Toxicol*. **2013**, 6(3):111-125. doi:10.2478/intox-2013-0019 (accessed March 10, 2022).

3. Abbasi, D. Synovium & Synovial Fluid. https://www.orthobullets.com/basic-science/9018/synovium-and-synovial-fluid (accessed March 10, 2022).

4. Bartok B and Firestein GS. Fibroblast-like synoviocytes: key effector cells in rheumatoid arthritis. *Immunol Rev*. **2010**, 233(1):233-255. doi:10.1111/j.0105-2896.2009.00859.x (accessed March 10, 2022).

5. Iwanaga T; Shikichi M; Kitamura H; etc. Morphology and functional roles of synoviocytes in the joint. *Arch Histol Cytol.* **2000**, 63(1):17-31. doi: 10.1679/aohc.63.17. PMID: 10770586. (accessed March 10, 2022).

6. Firestein, G. S. Invasive Fibroblast-like Synoviocytes in Rheumatoid Arthrtis. Passive Responders or Transformed Aggressors. *Arthritis Rheumology* **1996**, 39, 1781-1790. http://dx.doi.org/10.1002/art.1780391103 (accessed March 11, 2022).

7. Anatomy & Physiology, Synovial Joints. http://pressbooks-dev.oer.hawaii.edu/anatomyandphysiology/chapter/synovial-joints/ (accessd March 11, 2022).

8. Sophia Fox AJ; Bedi A and Rodeo S. A. The basic science of articular cartilage: structure, composition, and function. *Sports Health*. **2009**,1(6):461-468. doi:10.1177/1941738109350438 (accessed March 10, 2022).

9. Buckwalter J.A.; Mankin H.J. and Grodzinsky AJ. Articular cartilage and osteoarthritis. *Instr Course Lect*. **2005**, 54:465-80. PMID: 15952258. (accessed March 12, 2022).

10. Li, G.; Yin, J.; Gao, J.; etc. Subchondral bone in osteoarthritis: insight into risk factors and microstructural changes. *Arthritis Res Ther*. **2013**, 15**(**223). https://doi.org/10.1186/ar4405. (accessed March 13, 2022).

11. Säämänen, A.M.; Arokoski, J.P.A.; Jurvelin, J.S.; etc. The structure and regenerative capacity of synovial joints in *Regenerative Medicine and Biomaterials for the Repair of Connective Tissues*, Biomaterials; Woodhead Publishing, 2010; pp.1-39.

12. Mohamed AM. An overview of bone cells and their regulating factors of differentiation. *Malays J Med Sci*. **2008**,15(1):4-12. (accessed March 14, 2022).

13. Lean JM; Mackay AG; Chow JW; etc. Osteocytic expression of mRNA for c-fos and IGF-I: an immediate early gene response to an osteogenic stimulus. *Am J Physiol.* **1996**, 270:E937-45. doi: 10.1152/ajpendo.1996.270.6.E937. (accessed March 15, 2022).

14. Osteoarthritis (OA). https://www.cdc.gov/arthritis/basics/osteoarthritis.htm (accessed March 1, 2022).

15. Robinson WH; Lepus CM; Wang Q; etc. Low-grade inflammation as a key mediator of the pathogenesis of osteoarthritis. *Nat Rev Rheumatol*. **2016**, 12(10):580-592. doi:10.1038/nrrheum.2016.136 (accessed March 10, 2022).

16. Goldring MB and Goldring SR. Articular cartilage and subchondral bone in the pathogenesis of osteoarthritis. *Ann N Y Acad Sci*. **2010**,1192:230-237. doi:10.1111/j.1749-6632.2009.05240.x (accessed March 2, 2022).

17. Sellam J and Berenbaum F. The role of synovitis in pathophysiology and clinical symptoms of osteoarthritis. *Nat Rev Rheumatol*. **2010**, 6(11):625-635. doi:10.1038/nrrheum.2010.159 (accessed March 3, 2022).

18. Hunter DJ. Pharmacologic therapy for osteoarthritis--the era of disease modification. *Nat Rev Rheumatol*. **2011**, 7(1):13-22. doi:10.1038/nrrheum.2010.178 (accessed March 3, 2022).

19. Little CB and Hunter DJ. Post-traumatic osteoarthritis: from mouse models to clinical trials. *Nat Rev Rheumatol*. **2013**, 9(8):485-497. doi:10.1038/nrrheum.2013.72 (accessed March 4, 2022).

20. de Lange-Brokaar BJ; Kloppenburg M; Andersen SN; etc. Characterization of synovial mast cells in knee osteoarthritis: association with clinical parameters. *Osteoarthritis Cartilage*. **2016**, 24(4):664-671. doi:10.1016/j.joca.2015.11.011 (accessed March 5, 2022).

21. Kevorkian L; Young DA; Darrah C; etc. Expression profiling of metalloproteinases and their inhibitors in cartilage. *Arthritis Rheum*. **2004**, 50(1):131-141. doi:10.1002/art.11433 (accessed March 5, 2022).

22. Donell S. Subchondral bone remodelling in osteoarthritis. *EFORT Open Rev*. **2019**, 4(6):221-229. doi:10.1302/2058-5241.4.180102 (accessed March 8, 2022).

23. Henrotin Y; Pesesse L and Sanchez C. Subchondral bone and osteoarthritis: biological and cellular aspects. *Osteoporos Int*. **2012,** 23 Suppl 8:S847-S851. doi:10.1007/s00198-012-2162-z (accessed March 8, 2022).

24. Bellido M; Lugo L; Roman-Blas J.A; etc. Subchondral bone microstructural damage by increased remodelling aggravates experimental osteoarthritis preceded by osteoporosis. *Arthritis Res Ther*. **2010**, 12(4):R152. doi:10.1186/ar3103 (accessed March 9, 2022).

25. Henriksen K; Neutzsky-Wulff AV; Bonewald LF; etc. Local communication on and within bone controls bone remodeling. *Bone.* **2009**, doi: 10.1016/j.bone.2009.03.671.

26. Blom A.B; van Lent P.L; Holthuysen A.E; etc. Synovial lining macrophages mediate osteophyte formation during experimental osteoarthritis. *Osteoarthritis Cartilage*. **2004**, 12(8):627-635. doi:10.1016/j.joca.2004.03.003 (accessed March 9, 2022).

27. Choi MC; Jo J; Park J; etc. NF-κB Signaling Pathways in Osteoarthritic Cartilage Destruction. *Cells*. **2019**, 8(7):734. doi:10.3390/cells8070734 (accessed March 9, 2022).

28. Albensi BC. What Is Nuclear Factor Kappa B (NF-κB) Doing in and to the Mitochondrion?. *Front Cell Dev Biol*. **2019**, 7:154. doi:10.3389/fcell.2019.00154 (accessed March 10, 2022).

29. Nakamura H; Yoshino S; Kato T; etc. T-cell mediated inflammatory pathway in osteoarthritis. *Osteoarthritis Cartilage*. **1999**, 7(4):401-402. doi:10.1053/joca.1998.0224 (accessed March 4, 2022).

30. Blom A.B; van Lent PL; Libregts S; etc. Crucial role of macrophages in matrix metalloproteinase-mediated cartilage destruction during experimental osteoarthritis: involvement of matrix metalloproteinase 3. *Arthritis Rheum*. **2007**, 56(1):147-157. doi:10.1002/art.22337 (accessed March 5, 2022).

31. van Lent P.L; Blom A.B; van der Kraan P; etc. Crucial role of synovial lining macrophages in the promotion of transforming growth factor beta-mediated osteophyte formation. *Arthritis Rheum*. **2004**, 50(1):103-111. doi:10.1002/art.11422 (accessed March 10, 2022).

32. Vincent T.L.; Williams R.O.; Maciewicz R; etc. Mapping pathogenesis of arthritis through small animal models. *Rheumatology.* **2012**, 51(11): 1931-1941. doi: 10.1093/rheumatology/kes035. (accessed March 10, 2022).

33. Zeng C.Y.; Zhang Z.R.; Tang Z.M.; etc. Benefits and Mechanisms of Exercise Training for Knee Osteoarthritis. *Front Physiol.* **2021**, 12: 794062. doi: 10.3389/fphys.2021.794062 (accessed March 11, 2022).

34. Schaible H.G. and Grubb B.D. Afferent and spinal mechanisms of joint pain. *Pain*. **1993**, 55(1):5-54. doi:10.1016/0304-3959(93)90183-P (accessed March 10, 2022).

35. Perandini L.A; de Sá-Pinto A.L; Roschel H; etc. Exercise as a therapeutic tool to counteract inflammation and clinical symptoms in autoimmune rheumatic diseases. *Autoimmun Rev*. **2012**, 12(2):218-224. doi:10.1016/j.autrev.2012.06.007 (accessed March 9, 2022).

36. Petersen A.M and Pedersen B.K. The anti-inflammatory effect of exercise. *J Appl Physiol (1985)*. **2005**, 98(4):1154-1162. doi:10.1152/japplphysiol.00164.2004 (accessed March 9, 2022).

37. Henriksen M; Klokker L; Graven-Nielsen T; etc. Association of exercise therapy and reduction of pain sensitivity in patients with knee osteoarthritis: a randomized controlled trial. *Arthritis Care Res (Hoboken)*. **2014**, 66(12):1836-1843. doi:10.1002/acr.22375 (accessed March 9, 2022).

38. Musumeci G; Castrogiovanni P; Trovato FM; etc. Physical activity ameliorates cartilage degeneration in a rat model of aging: a study on lubricin expression. *Scand J Med Sci Sports*. **2015**, 25(2):e222-e230. doi:10.1111/sms.12290 (accessed March 9, 2022).

39. Iijima H; Ito A; Nagai M; etc. Physiological exercise loading suppresses post-traumatic osteoarthritis progression via an increase in bone morphogenetic proteins expression in an experimental rat knee model. *Osteoarthritis Cartilage*. **2017**, 25(6):964-975. doi:10.1016/j.joca.2016.12.008 (accessed March 10, 2022).

40. Yang Y; Wang Y; Kong Y; etc. Mechanical stress protects against osteoarthritis via regulation of the AMPK/NF-κB signaling pathway. *J Cell Physiol*. **2019**, 234(6):9156-9167. doi:10.1002/jcp.27592 (accessed March 9, 2022).

41. Pitcher M.H; Tarum F; Rauf I.Z; etc. Modest Amounts of Voluntary Exercise Reduce Pain- and Stress-Related Outcomes in a Rat Model of Persistent Hind Limb Inflammation [published correction appears in J Pain. **2017**;18(8):1016]. *J Pain*. **2017**;18(6):687-701. doi:10.1016/j.jpain.2017.01.006 (accessed March 10, 2022).

42. Kawanishi N; Yano H; Yokogawa Y; etc. Exercise training inhibits inflammation in adipose tissue via both suppression of macrophage infiltration and acceleration of phenotypic switching from M1 to M2 macrophages in high-fat-diet-induced obese mice. *Exerc Immunol Rev*. **2010**, 16:105-118. (accessed March 10, 2022).

43. Wang J; Song H; Tang X; etc. Effect of exercise training intensity on murine T-regulatory cells and vaccination response. *Scand J Med Sci Sports*. **2012**, 22(5):643-652. doi:10.1111/j.1600-0838.2010.01288.x (accessed March 10, 2022).

44. Cerqueira É; Marinho D.A; Neiva H.P; etc. Inflammatory Effects of High and Moderate Intensity Exercise-A Systematic Review. *Front Physiol*. **2020**,10:1550. doi:10.3389/fphys.2019.01550 (accessed March 10, 2022).

45. Koelwyn G.J; Wennerberg E; Demaria S; etc. Exercise in Regulation of Inflammation-Immune Axis Function in Cancer Initiation and Progression. *Oncology (Williston Park)*. **2015**, 29(12):908-922. (accessed March 10, 2022).

46. Siebelt M; Groen H.C; Koelewijn S.J; etc. Increased physical activity severely induces osteoarthritic changes in knee joints with papain induced sulfate-glycosaminoglycan depleted cartilage. *Arthritis Res Ther*. **2014**, 16(1):R32. doi:10.1186/ar4461 (accessed March 10, 2022).

47. Cifuentes D.J; Rocha L.G; Silva L.A; etc. Decrease in oxidative stress and histological changes induced by physical exercise calibrated in rats with osteoarthritis induced by monosodium iodoacetate. *Osteoarthritis Cartilage*. **2010**,18(8):1088-1095. doi:10.1016/j.joca.2010.04.004 (accessed March 10, 2022).

48. Nicolson P.J.A; Hinman R.S; Kasza J; etc. Trajectories of adherence to home-based exercise programs among people with knee osteoarthritis. *Osteoarthritis Cartilage*. **2018**, 26(4):513-521. doi:10.1016/j.joca.2018.01.009 (accessed March 10, 2022).

49. Bendele A.M. Animal models of osteoarthritis. *J Musculoskelet Neuronal Interact*. **2001**,1(4):363-376.

50. Iijima H; Aoyama T; Ito A; etc. Effects of short-term gentle treadmill walking on subchondral bone in a rat model of instability-induced osteoarthritis. *Osteoarthritis Cartilage*. **2015**, (9):1563-74. doi: 10.1016/j.joca.2015.04.015. (accessed March 19, 2022).

51. Saito R; Muneta T; Ozeki N; etc. Strenuous running exacerbates knee cartilage erosion induced by low amount of mono-iodoacetate in rats. *BMC Musculoskelet Disord*. **2017**,18(1):36. doi: 10.1186/s12891-017-1393-8. (accessed March 19, 2022).

52. Bijlsma JW; Berenbaum F; Lafeber FP. Osteoarthritis: An update with relevance for clinical practice. *Lancet.* **2011**; 377(9783): 2115-2126. doi: 10.1016/S0140-6736(11)60243-2 (accessed April 5, 2022).

53. Wenham CYJ and Conaghan PG. The Role of Synovitis in Osteoarthritis. *Ther Adv Musculoskelet Dis.* **2010**; 2(6): 349-359. doi: 10.1177/1759720X10378373 (accessed April 6, 2022).

54. Kraus VB; McDaniel G; Huebner JL; etc. Direct in vivo evidence of activated macrophages in human osteoarthritis. *Osteoarthritis Cartilage.* **2016;** 24: 1613-1621. DOI: 10.1016/j.joca.2016.04.010 (accessed March 17, 2022).

55. Saito I; Koshino T; Nakashima K; etc. Increased cellular infiltrate in inflammatory synovia of osteoarthritic knees. *Osteoarthritis Cartilage*. **2002**; 10(2):156-162. doi:10.1053/joca.2001.0494 (accessed March 12, 2022).

56. Xie J; Huang Z; Yu X; etc. Clinical implications of macrophage dysfunction in the development of osteoarthritis of the knee. *Cytokine and Growth Factor Reviews*. **2019**; 46: 36-44. doi: 10.1016/j.cytogfr.2019.03.004 (accessed April 5, 2022).

57. Thomson A and Hilkens CMU. Synovial Macrophages in Osteoarthritis: The Key to Understanding Pathogenesis? *Front. Immunol*. **2021**; 12:678757. doi: 10.3389/fimmu.2021.678757 (accessed March 16, 2022).

58. Roemer FW; Kwoh CK; Hannon MJ; etc. What comes first? Multitissue involvement leading to radiographic osteoarthritis: magnetic resonance imaging based trajectory analysis over four years in the osteoarthritis initiative. *Arthritis Rheumatol.* **2015**;67:208596.35 doi:10.1002/art.39176 (accessed March 16, 2022).

59. Weber A; Chan PMB; Wen C. Do immune cells lead the way in subchondral bone disturbance in osteoarthritis? *Prog Biophys Mol Biol.* **2019**; 148: 21-31. doi: 10.1016/j.pbiomolbio.2017.12.004. (accessed March 13, 2022).

60. Hunter DJ; Gerstenfeld L; Bishop G; etc. Bone marrow lesions from osteoarthritis knees are characterized by sclerotic bone that is less well mineralized. *Arthritis Res Ther.* **2009**;11: R11. doi: 10.1186/ar2601. (accessed March 19, 2022).

61. Burr DB and Gallant MA. Bone remodelling in osteoarthritis. *Nat Rev Rheumatol*. **2012**; 8(11):665-73. doi: 10.1038/nrrheum.2012.130.

62. Hügle T and Geurts J.What drives osteoarthritis? - synovial versus subchondral bone pathology. *Rheumatology (Oxford).* **2017***;* 56(9):1461-1471. doi: 10.1093/rheumatology/kew389. (accessed March 19, 2022).

63. Berardi S; Corrado A; Maruotti N; etc. Osteoblast role in the pathogenesis of rheumatoid arthritis. *Mol Biol Rep.* **2021;** 48**:** 2843–2852. doi: 10.1007/s11033-021-06288-y. (accessed March 19, 2022).

64. Adamopoulos IE; Sabokbar A; Wordsworth BP; etc. Synovial fluid macrophages are capable of osteoclast formation and resorption. *J Pathol*. **2006**; 208(1):35-43. doi: 10.1002/path.1891 (accessed March 19, 2022).

65. Danks L; Sabokbar A; Gundle R; etc. Synovial macrophage-osteoclast differentiation in inflammatory arthritis. *Ann Rheum Dis*. **2002**; 61(10):916-21. doi: 10.1136/ard.61.10.916 (accessed March 20, 2022).

66. Van der Kraan PM and van den Berg WB. Review Osteophytes: relevance and biology. *Osteoarthritis and Cartilage*. **2007**; 15(3): 237-244. doi:10.1016/j.joca.2006.11.006 (accessed March 20, 2022).

67. Blom AB; van Lent PL; Holthuysen AE; etc. Synovial lining macrophages mediate osteophyte formation during experimental osteoarthritis. *Osteoarthritis Cartilage*. **2004**;12(8):627-35. doi: 10.1016/j.joca.2004.03.003 (accessed March 20, 2022).

68. Bondeson J; Wainwright SD; Lauder S; etc. (2006) The role of synovial macrophages and macrophage-produced cytokines in driving aggrecanases, matrix metalloproteinases, and other destructive and inflammatory responses in osteoarthritis. *Arthritis Res Ther*. **2006**; 8:187. doi: 10.1186/ar2099 (accessed March 17, 2022).

69. Berkelaar MHM; Korthagen NM; Jansen G; etc. Synovial Macrophages: Potential Key Modulators of Cartilage Damage, Osteophyte Formation and Pain in Knee Osteoarthritis. *J Rheum Dis Treat*. **2018**; 4(1): 1-16. DOI: 10.23937/2469-5726/1510059 (accessed March 10, 2022).

70. Wang N; Liang H; Zen K; Molecular mechanisms that influence the macrophage M1-M2 polarization balance. *Front Immunol*. **2014**; 5:614. doi: 10.3389/fimmu.2014.00614 (accessed April 4, 2022).

71. Wang LX; Zhang SX; Wu HJ; etc. M2b macrophage polarization and its roles in diseases. *J Leukoc Biol.* **2019**; 106(2): 345-358. doi: 10.1002/JLB.3RU1018-378RR (accessed March 19, 2022).

72. de Lange-Brokaar BJE; Ioan-Facsinay A; van Osch GJVM; etc. Synovial inflammation, immune cells and their cytokines in osteoarthritis. *Osteoarthritis Cartilage*. **2012**; 20(12):1484-1499. doi: 10.1016/j.joca.2012.08.027 (accessed March 15, 2022).

[73] Utomo L; van Osch GJVM; Bayon Y; etc. Guiding synovial inflammation by macrophage phenotype modulation: an in vitro study towards a therapy for osteoarthritis. *Osteoarthritis Cartilage*. **2016**; 24(9):1629-1638. doi: 10.1016/j.joca.2016.04.013 (accessed March 15, 2022).

74. Kawasaki T and Kawai T. Toll-like receptor signaling pathways. *Front. Immunol.* **2014**; 5:461. doi: 10.3389/fimmu.2014.00461 (accessed March 19, 2022).

75. Nair, A; Kanda V; Bush-Joseph C; etc. Synovial fluid from patients with early osteoarthritis modulates fibroblast-like synoviocyte responses to Toll-like receptor 4 and Toll-like receptor 2 ligands via soluble CD14. *Osteoarthritis*. **2012**; 64(7):2268-2277. doi: 10.1002/art.34495 (accessed March 14, 2022).

76. Molteni M; Gemma S; Rossetti C. The Role of Toll-Like Receptor 4 in Infectious and Noninfectious Inflammation. *Mediators Inflamm*. **2016**; 2016:6978936. doi: 10.1155/2016/6978936 (accessed March 14, 2022).

77. Oliveira-Nascimento L; Massari P; Wetzler LM. The role of TLR2 in infection and immunity. *Front. Immunol.* **2012**; 3:79. doi: 10.3389/fimmu.2012.00079 (accessed March 14, 2022).

78. Lambert C; Zappia J; Sanchez C; etc. The Damage-Associated Molecular Patterns (DAMPs) as Potential Targets to Treat Osteoarthritis: Perspectives From a Review of the Literature. *Front Med (Lausanne)*. **2021**; 7:607186. doi:10.3389/fmed.2020.607186 (accessed March 10, 2022).

[79] Miller RE; Scanzello CR; Malfait AM. An Emerging Role for Toll-like Receptors at the Neuroimmune Interface in Osteoarthritis. *Semin Immunopathol.* **2019**; 41(5): 583-594. doi:10.1007/s00281-019-00762-3 (accessed March 16, 2022).

80. Hanaoka R; Kasama T; Muramatsu M; etc. A novel mechanism for the regulation of IFN-gamma inducible protein-10 expression in rheumatoid arthritis. *Arthritis Res Ther*. **2003**, 5(2):R74-R81. doi:10.1186/ar616 (accessed March 12, 2022).

81. T Helper 1 Cells Overview. https://www.thermofisher.com/us/en/home/life-science/cell-analysis/cell-analysis-learning-center/immunology-at-work/t-helper-1-cell-overview.html#:~:text=What%20are%20Th1%20cells%3F,for%20their%20activation%20and%20maturation. (accessed March 10, 2022).

82. Saetan N; Honsawek S; Tanavalee A; etc. Association of plasma and synovial fluid interferon-γ inducible protein-10 with radiographic severity in knee osteoarthritis. *Clin Biochem*. **2011**, 44(14-15):1218-1222. doi:10.1016/j.clinbiochem.2011.07.010 (accessed March 10, 2022).

83. Lee JH; Kim HN; Kim KO; etc. CXCL10 promotes osteolytic bone metastasis by enhancing cancer outgrowth and osteoclastogenesis. *Cancer Res*. **2012**, 72(13):3175-3186. doi:10.1158/0008-5472.CAN-12-0481 (accessed March 13, 2022).

84. Kwak HB; Ha H; Kim HN; etc. Reciprocal cross-talk between RANKL and interferon-gamma-inducible protein 10 is responsible for bone-erosive experimental arthritis. *Arthritis Rheum*. **2008**, 58(5):1332-1342. doi:10.1002/art.23372 (accessed March 13, 2022).

85. Lee EY; Lee ZH and Song YW. CXCL10 and autoimmune diseases. *Autoimmun Rev*. **2009**, 8(5):379-383. doi:10.1016/j.autrev.2008.12.002 (accessed March 14, 2022).

86. Mödinger Y; Rapp A; Pazmandi J; etc. C5aR1 interacts with TLR2 in osteoblasts and stimulates the osteoclast-inducing chemokine CXCL10. *J Cell Mol Med*. **2018**, 22(12):6002-6014. doi:10.1111/jcmm.13873 (accessed March 13, 2022).

87. Souza PPC and Lerner UH. Finding a Toll on the Route: The Fate of Osteoclast Progenitors After Toll-Like Receptor Activation. *Front Immunol.* **2019**; 10:1663. doi: 10.3389/fimmu.2019.01663 (accessed March 14, 2022).

88. Kassem A; Lindholm C; Lerner UH. Toll-Like Receptor 2 Stimulation of Osteoblasts Mediates Staphylococcus Aureus Induced Bone Resorption and Osteoclastogenesis through Enhanced RANKL. *PLoS One.* **2016**; 11(6):e0156708. doi: 10.1371/journal.pone.0156708 (accessed March 14, 2022).

89. Cavalcante PAM; Gregnani MF; Henrique JS; etc. Aerobic but not Resistance Exercise can induce inflammatory pathways via Toll-Like 2 and 4: a Systematic Review. *Sports Med Open.* **2017**; 3(1):42. doi: 10.1186/s40798-017-0111-2 (accessed March 14, 2022).

90. Flynn MG; McFarlin BK; Phillips MD; etc. Toll-like receptor 4 and CD14 mRNA expression are lower in resistive exercise-trained elderly women. *J Appl Physiol (1985)*. **2003**; 95(5):1833-1842. doi:10.1152/japplphysiol.00359.2003 (accessed March 14, 2022).

91. Kawanishi N; Yano H; Mizokami T; etc. Mechanisms of chronic inflammation improvement by exercise: Focus on immune response of local tissue. *J Sports Med Phys Fitness*. **2013**, 2(4):487-492. https://doi.org/10.7600/jpfsm.2.487 (accessed March 13, 2022).